UNIVERSITEIT VAN PRETORIA
UNIVERSITY OF PRETORIA
YUNIBESITHI YA PRETORIA

Continuous cell recycle succinic acid fermentation by *Escherichia coli* KJ 122

by

Adolf Krige

Dissertation presented in partial fulfilment of the requirements for the degree

Master of Engineering in Chemical Engineering

at the University of Pretoria

Faculty of Engineering, Built Environment and Information Technology

Department of Chemical Engineering

University of Pretoria

Supervisor: Prof. W. Nicol

January 2015

Notice: The respective chapters, sections, figures, tables and equations within the study are cross-referenced through hyperlinks within the portable document format (pdf) document. Any hyper-links within the text are indicated by blue formatting (e.g. Figure 2-1) and clicking on these links within the text will redirect the reader to the referenced item. Within the software package “Adobe Acrobat Reader”, the reader can return to the original hyper-link from which the link was referenced by either selecting the “Previous view” icon on the toolbar, or by simultaneously depressing the alt and the left arrow keys on the key-board.

Synopsis

The effectiveness of the genetically modified *E. coli* strain KJ 122 with regard to succinic acid (SA) production was evaluated under high cell density fermentation conditions in a continuous cell recycle reactor equipped with a hollow fibre filter. Batch fermentations were performed in a standard 1,5 L bioreactor for the purposes of comparison and to investigate the productivity, yield and titre that could be obtained.

Continuous cell recycle fermentation led to a significant increase in volumetric productivity when compared with batch fermentations, albeit at a lower SA titre. The highest continuous volumetric productivity of 3 g/L/h was achieved at the highest dilution rate (0.15 h^{-1}), at an SA titre of 19 g/L, which was five times higher than the overall batch productivity. The batch fermentations did, however, reach a final SA titre of 56 g/L. Unfortunately, severe product inhibition, at SA concentrations above 25 g/L, makes continuous production at high titres unfeasible and limits the cellular concentration in the fermenter due to cell death and subsequent cell lysis. Therefore, although temporary high dry cell weight was achieved, the biomass died off until an equilibrium was established between the cell growth, cell death and cells removed through the bleed stream.

The SA yields obtained during batch fermentation (0.85 g/g glucose) were, however, superior to those obtained during continuous cell recycle fermentations (0.69 to 0.77 g/g). This was due mainly to the utilisation of pyruvate and formate at high SA titres during the latter part of the batch fermentations.

The SA yield did, however, increase as the dilution rate increased, with the maximum yield (0.77 g/g) being obtained at a dilution rate of 0.15 h^{-1}. Based on the metabolic flux analysis, this is believed to be due to an increase in pyruvate dehydrogenase activity at higher dilution rates. This increase led to a decrease in pyruvate and formate concentrations, and an increase in the flux through the reductive branch of the tricarboxylic acid cycle (due to the additional nicotinamide adenine dinucleotide produced).

Low titres would increase the downstream processing requirements. To evaluate the economic feasibility of high cell density fermentation, the low titres and high productivities of continuous cell recycle fermentation would therefore have to be evaluated against the lower productivities and higher titres of batch fermentations.

Keywords: Succinic acid, *Escherichia coli*, Cell recycle, Metabolic flux analysis

Contents

Synopsis i

List of figures iii

List of tables iv

Abbreviations v

Nomenclature vi

1 Introduction 1

1.1 Study objective 3

2 Theory 4

2.1 Succinic acid 4

2.2 *Escherichia coli* 5

2.3 Biochemistry and yields of glucose-to-succinate conversion 6

2.4 Cell recycling 10

2.4.1 Membrane devices 12

2.4.2 Filter system design criteria 13

3 Experimental 15

3.1 Microorganisms and inoculums 15

3.2 Fermentation medium 15

3.3 Bioreactor 16

3.3.1 Membrane criteria selection and cell recycle operation 19

3.4 Fermentation 23

3.5 Analytical methods 24

3.5.1 High-performance liquid chromatography (HPLC) 24

3.5.2 Dry cell weight (DCW) 25

3.6 Data analysis 25

3.6.1 Batch analysis protocol 25

3.6.2 Definition of steady state 26

3.6.3 Metabolic flux analysis 26
3.6.4 Mass balance 29
4 Results and discussion 30
4.1 Batch fermentation results 30
4.2 Continuous fermentation results 32
4.3 Metabolic flux analysis of continuous fermentations 36
4.4 Discussion 37
4.4.1 Cell growth and viability 37
4.4.2 Comparison with previous studies 39
4.4.3 Metabolic product distribution 40
4.4.4 Productivity: Batch fermentation compared with continuous fermentation 41
5 Conclusions 43
6 References 45

List of figures

Figure 2-1: Succinic acid, with chemical formula $C_4H_6O_4$ 4
Figure 2-2: Simplified metabolic pathways of (A) native SA producers, and (B) genetically modified *E. coli* 7
Figure 2-3: Standard pathway for the metabolism of glucose in *E. coli* 9
Figure 3-1: Schematic of the reactor setup for batch fermentations 17
Figure 3-2: Reactor equipped for cell recycling 23
Figure 3-3: Simplified metabolic pathways for the anaerobic metabolism of glucose in *E. coli* 27
Figure 4-1: Concentration profiles of three separate batch runs, showing the repeatability of the runs 31
Figure 4-2: Concentration profiles of the byproducts pyruvate and formate, showing the decrease in concentration as the fermentation proceeds 31
Figure 4-3: SA productivity of the batch fermentations, showing the decrease in productivity as the SA increases 32
Figure 4-4: Continuous fermentation results, showing the glucose consumed, succinic acid concentration and DCW concentration 34
Figure 4-5: Continuous fermentation byproduct results, showing the acetic, pyruvic and formic acid concentrations 34
Figure 4-6: KOH dosing rate used in determining whether sample points can be considered as steady state 35
Figure 4-7: Average metabolite concentrations from the continuous cell recycle fermentations 36
Figure 4-8: SA productivity during the continuous cell recycle fermentation 36

List of tables

Table 2-1: The relevant gene modifications made to *E. coli* C 8
Table 3-1: *E. coli* AM1 defined fermentation medium composition, with concentrated salt solution composition 16
Table 3-2: Summary of previous continuous cell recycle studies using hollow fibre filters 21
Table 4-1: Differences in batch fermentations performed 30
Table 4-2: Final concentration of metabolites produced during batch fermentations, with the resulting yields 31
Table 4-3: Average continuous fermentation results at different dilution rates, with standard deviation 35
Table 4-4: Results from metabolic flux analysis 37

Abbreviations

AA	Acetic acid
ATP	Adenosine triphosphate
CTA	Cellulose tri-acetate
DCW	Dry cell weight
FA	Formic acid
HCDF	High cell density fermentation
HFF	Hollow fibre filter
HPLC	High-performance liquid chromatography
LA	Lactic acid
LBB	Luria-Bertani broth
MFT	Maximum fermentation time
NADH	Nicotinamide adenine dinucleotide
NMWC	Nominal molecular weight cut-off
OD	Optical density
PA	Pyruvic acid
PEP	Phosphoenolpyruvate
PP	Polypropylene
PS	Polysulphone
SA	Succinic acid
TCA	Tricarboxylic acid cycle
TMP	Transmembrane pressure

Nomenclature

A	Membrane area	[m^2]
AccKOH	Accumulated KOH dosing volume	[L]
$ACoA_{cit}$	Fraction of acetyl-CoA converted to isocitrate instead of acetate	[cmol/cmol]
C_i	Concentration of metabolite 'i' during batch fermentation	[g/L]
C_i^*	Correction of metabolite concentration 'i'	[g/L]
J	Filtrate flux	[L/m^2h]
M_i	Mass of metabolite 'i' produced during batch fermentation	[g]
PEP_{pyr}	Fraction of PEP converted to pyruvate instead of oxaloacetate	[cmol/cmol]
P_{TMP}	Transmembrane pressure	[kPa]
Pyr_{out}	Fraction of pyruvate excreted instead of converted to acetyl-CoA	[cmol/cmol]
Pyr_{pdh}	Fraction of pyruvate converted to acetyl-CoA through pyruvate dehydrogenase instead of through pyruvateformate-lyase	[cmol/cmol]
r/s	Recirculation rate per membrane area	[cm/h]
s/v	Membrane area per volume of reactor	[cm^{-1}]
t=0	Used to indicate reactor starting conditions	[-]
V	Reactor volume	[L]
Y_{SA}	Acetic acid yield per glucose consumed	[g/g]
Y_{SP}	Succinic acid yield per glucose consumed	[g/g]

1 Introduction

Classical sources such as petroleum oil and natural gas produce the fundamental materials on which the modern industrial chemical industry is based. Climate change, the limited availability of these resources, and the increasing demand and price of fossil fuels have led to a demand for a sustainable and economically viable alternative (Muffler & Ulber, 2008). The production of alternative bio-based chemicals has therefore become significantly more desirable. Biotechnology is a fast-growing field that has the potential to influence the production of fuels and chemicals significantly. The concept of a biorefinery has recently become more attractive due to the decreasing popularity of fossil fuels, and has already been shown to be economically viable for the production of lactic acid (LA) and 1,3-propanediol (Sheldon, 2011).

The production of organic acids forms a significant portion of the biochemical industry. Some organic acids, that can be produced using microorganisms, have potential as building-block molecules in the chemical industry due to the functional groups present in these acids (Jantama *et al*., 2008). Succinic acid (SA) is considered one of the top sugar-derived, building-block chemicals, which can be converted to several higher-value products (Werpy & Petersen, 2004). Several microorganisms have been found to produce SA, including *Actinobacillus succinogenes, Mannheimia succiniciproducens, Anaerobiospirillum succiniciproducens* and various strains of modified *Escherichia coli* (Van Heerden & Nicol, 2013).

During anaerobic fermentation, the naturally producing organisms produce SA via the reverse tricarboxylic acid (TCA) cycle, yet this is a reductive pathway that requires the consumption of nicotinamide adenine dinucleotide (NADH). Naturally producing organisms therefore require an oxidative pathway to produce the required NADH and the organisms therefore have to produce other byproducts, usually acetic acid (AA), which significantly lowers the yields that can be obtained. One of the large advantages of the modified *E. coli* strains is that they contain the oxidative branch of the TCA cycle, which allows the organisms to produce NADH with SA as the final product. This could, theoretically, remove the need for any byproduct formation, thus

significantly increasing the SA yield. The *E. coli* strains also contain a glyoxylate cycle which could be used similarly, resulting in the same theoretical yield, although the glyoxylate shunt is active mainly under aerobic conditions (Van Heerden & Nicol, 2013). Some modified *E. coli* strains, such as *E. coli* KJ 122 and KJ 134, have shown promise as biocatalysts for the commercial production of SA, obtaining yields of up to 86% and 89%, respectively, of the theoretical SA yield (Jantama *et al*., 2008).

Genetic engineering has historically placed emphasis on high-value, low-volume products, such as pharmaceutical proteins, requiring significant downstream purification due to regulatory standards. In a biorefinery the emphasis will be on low-value, high-volume products such as ethanol, succinic acid and lactic acid. The productivity and yield of the bioreactors will therefore play a crucial role in ensuring the feasibility of the biorefinery (Chang, Yoo & Kim, 1994).

High productivities, yields and product titres will be required to minimise capital cost and downstream processing requirements. Unfortunately high titres typically lead to lower cell productivity, decreasing the volumetric productivity. By concentrating the cells in a continuous bioreactor, high titres can be achieved while achieving higher throughputs, resulting in higher volumetric productivities in spite of the lower cell productivity (Chang, Yoo & Kim, 1994). Utilising modified *E. coli* strains that could achieve high yields under high cell density fermentation (HCDF) conditions could therefore significantly increase the volumetric productivities that can be achieved.

Typical methods that have been used to increase the cell concentration include multi-stage fermentation, immobilisation, fed-batch cultures and cell recycle. Fed-batch cultures are by definition not suitable for continuous production, yet this is a common method in commercial practices. Since fed-batch cultures allow for the control of substrate concentrations, higher cell densities than those of batch cultures are possible, without ever having high substrate concentrations. The immobilisation, cell recycle and multi-stage fermentation methods are all suitable for continuous operation. Operation at high dilution rates can lead to cell washout with other continuous methods, but the immobilisation and cell recycle methods do permit operation at high dilution rates, thus increasing productivity. Although immobilisation techniques allow for high cell densities, the method typically has scale-up difficulties,

poor nutrient transfer rates and low overall productivity per cell (Chang, Yoo & Kim, 1994; Toda, 2003)

Meynial-Salles, Dorotyn and Soucaille (2008) reported an SA production rate of 14.8 g/L/h using *A. succiniciproducens* in a membrane cell recycle reactor, which was almost five times higher than the production rate in studies using the same organism in continuous bioreactors without cell recycle (Beauprez, De Mey & Soetaert, 2010).

1.1 Study objective

The objective of this study was to investigate the performance (with regard to SA production) of a genetically modified strain of *E. coli* (KJ 122) under HCDF conditions, in a cell recycle reactor. The key factors investigated were the titre, yield and productivity that could be obtained in a cell recycle reactor. Metabolic flux analysis was used to better understand the samples from continuous cell recycle fermentations. Batch runs were undertaken to serve as a comparison for yields and titres, as well as to evaluate or explain the HCDF results.

Succinic acid was produced using D-glucose as the main substrate in a minimal medium. The fermentation took place in a standard laboratory-scale bioreactor, using a recycle line equipped with an external hollow fibre filter to extract the medium and recycle the cells back into the reactor. The pH and temperature were controlled at 6.8 and 37 °C respectively, and the steady state was evaluated at different dilution rates. Batch runs were undertaken in the same reactor but with the cell recycle equipment removed.

2 Theory

2.1 Succinic acid

Succinic acid (SA), also known as amber acid, is a diprotic, dicarboxylic acid (Figure 2-1) and is considered to be one of the most important bio-based chemicals, according to the U.S. Department of Energy (Werpy & Petersen, 2004). SA can be seen as a platform chemical, since it can be used as a precursor of many industrially important chemicals, such as 1,4-butanediol, tetrahydrofuran, N-methyl pyrrolidinone, 2-pyrrolidinone and succinate salts. SA has recently also been used to synthesise biodegradable polymers such as polybutyrate succinate and polyamides (Song & Lee, 2006). Currently, the main uses of SA are in the detergent/surfactant market, the ion chelator market, the food market and the pharmaceutical market (Beauprez *et al*., 2010).

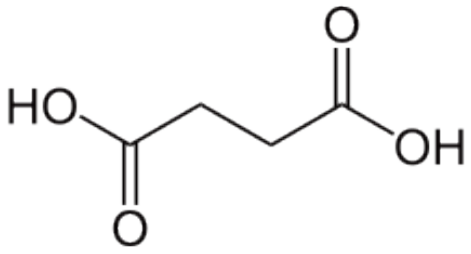

Figure 2-1: Succinic acid, with chemical formula $C_4H_6O_4$

Most industrial SA is currently being produced via maleic-anhydride using liquefied petroleum gas or petroleum oil as a starting material. There is, however, a high cost associated with the conversion of maleic anhydride to SA, limiting the applications. Analysis has, however, shown that the production of SA via the fermentation of renewable resources can be more cost-effective than via traditional processes (Song & Lee, 2006). The SA market is currently around 30-50 kton/year and recent applications could lead to a market in the order of megatons per annum. Several companies (such as Myriant, BioAmber, Succinity and Reverdia) have started, or are about to start, producing industrially significant quantities of bio-based SA to fill the gap in the growing SA market (Jansen & Van Gulik, 2014).

Bio-based SA is produced through the use of a microbial catalyst (biocatalyst) to convert carbohydrate substrates to SA. These biocatalysts can be categorised into natural producers and genetically modified biocatalysts.

Natural producers such as rumen bacteria (*Actinobacillus succinogenes, Anaerobiospirillum succiniciproducens, Mannheimia succiniciproducens* and *Bacillus fragilis*) and certain fungi (such as Fusarium, Aspergillus and Penicillium species) have shown promise in SA production, but natural strains tend to require complex nutrients to grow, increasing the cost of fermentation (Lin, Bennett & San, 2005; Jansen & Van Gulik, 2014).

Metabolic engineering has also been successfully applied to well-known industrial microorganisms (such as *E. coli, Corynebacterium glutamicum* or *Saccharomyces cerevisiae*), some of which are being used by companies starting large-scale fermentative production (Jansen & van Gulik, 2014).

2.2 *Escherichia coli*

Genetically modified *E. coli* strains have been developed that produce succinic acid in a minimal salt medium without the need for complex nutrients (Zhang *et al*., 2009). These strains also have the important benefit of increasing the succinate yields, up to a point close to the theoretical maximum (this is discussed further in Section 2.3).

E. coli is a Gram-negative, facultatively anaerobic, rod-shaped bacterium of the genus Escherichia. Under anaerobic growth, wild strains of *E. coli* generate mostly formate, lactate and ethanol, since the phosphoenolpyruvate (PEP) and pyruvate formed are converted through the Embden-Meyerhof-Parnas pathway (Vemuri, Eiteman & Altman, 2002a). These strains produce mixed acids under anaerobic growth, with small amounts of succinate. Genetic manipulation is therefore required to increase the succinate yield (Vemuri, Eiteman & Altman, 2002b).

A modified strain of *E. coli* (KJ 122) was developed by the Department of Microbiology and Cell Science of the University of Florida, U.S. This strain was based on derivatives of *E. coli* C, which produces succinic acid in a minimal salt medium. The strain was further enhanced by gene deletion after the source of the side-products acetate, malate and pyruvate had been identified. The relevant gene modifications are given later in Table 2-1, Section 2.3, along with the biochemistry of

succinate production, in order to explain the impact of the modifications (Jantama *et al*., 2008).

2.3 Biochemistry and yields of glucose-to-succinate conversion

The maximum stoichiometric SA yield can be determined from a redox balance, if one assumes that SA and water are the only products and that glucose and CO_2 are the only substrates, implying zero biomass growth. The maximum stoichiometric SA yield can be defined by Equation 1, and this equation results in a maximum SA yield, per gram of glucose consumed, of 1.12 g/g.

$$Gluc + \frac{6}{7}CO_2 \rightarrow \frac{12}{7}SA + \frac{6}{7}H_2O \quad (1)$$

However, to obtain the maximum theoretical yield the organisms require metabolic pathways that can achieve the stoichiometric result. Metabolic pathways are used to describe the enzymatic reactions that occur in an organism; NADH can be seen as a reductive power currency for the catabolism of glucose, allowing for the transfer of electrons between intermediate molecules (Nielsen, Villadsen & Lidén, 2011: 18).

In order to better explain the strategy behind high-yield SA-producing *E. coli* strains, a comparison can be made with naturally producing organisms. A comparison between the metabolic pathways of naturally producing organisms and genetically modified *E. coli* is shown in Figure 2-2.

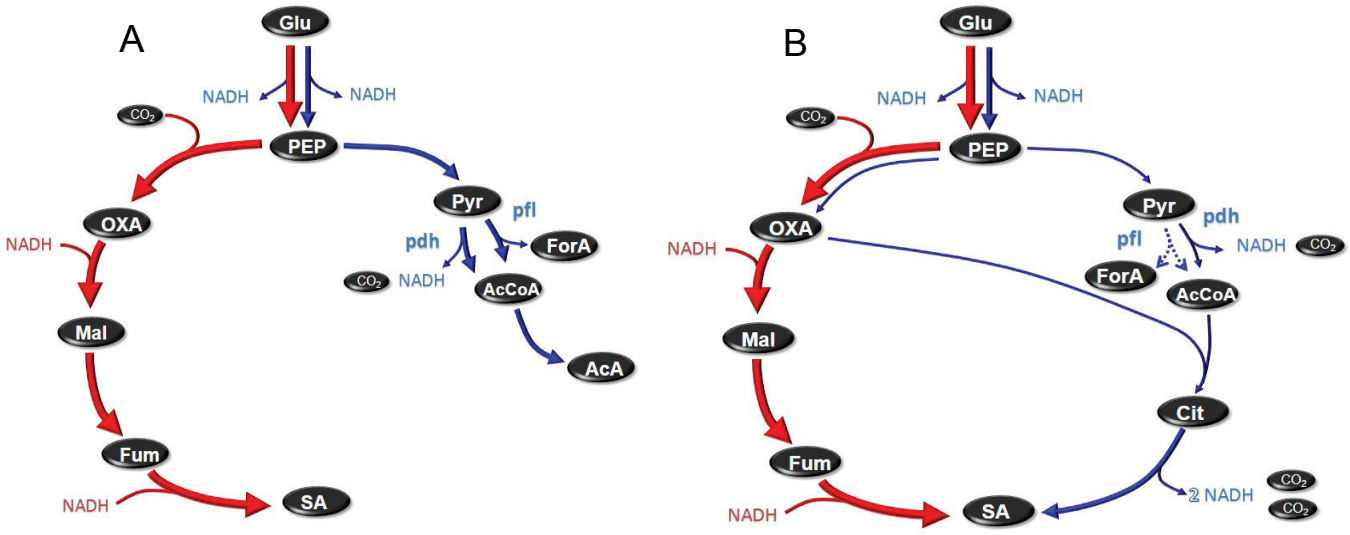

Key: AcA: acetate; AcCoA: acetyl coenzyme A; Cit: citric acid; ForA: formate; Fum: fumarate; Glu: glucose; Mal: malate; OXA: oxaloacetate; PEP: phosphoenolpyruvate; Pyr: pyruvate; SA: succinate

Figure 2-2: Simplified metabolic pathways of (A) native SA producers, and (B) genetically modified *E. coli*. Both pyruvate oxidation pathways are shown, via pyruvate formate lyase (*pfl*) and via pyruvate dehydrogenase (*pdh*).The figure shows how the genetically modified *E. coli* can obtain higher SA yields

However, naturally SA-producing bacteria such as *A. succinogenes* usually lack a complete TCA cycle that could produce NADH and therefore need to produce a byproduct such as acetic acid in order to balance the NADH consumed (shown in Figure 2-2 A). This therefore decreases the maximum possible SA yield. For *A. succinogenes* the maximum yield also depends on whether the pyruvateformate-lyase pathway, or the pyruvate dehydrogenase pathway, is active since pyruvate dehydrogenase produces an additional NADH molecule. The maximum yield of *A. succinogenes* using the pyruvateformate-lyase pathway can be calculated as 0.66 g/g and this changes to 0.87 g/g when pyruvate dehydrogenase is active (Van Heerden & Nicol, 2013). As can be seen, these yields fall far below the maximum stoichiometric yield of 1.12 g/g. Some genetically modified *E. coli* strains do contain metabolic pathways through which it could be possible to produce SA without byproducts (shown in Figure 2-2 B).

E. coli KJ 122 has been modified to obtain the highest possible SA yield. The standard metabolic pathways for the metabolism of glucose to various products by *E. coli* are given in Figure 2-3 and the relevant gene modifications are given in Table 2-1. To reduce byproduct formation, the genes for the anaerobic fermentative pathways that produce other products have been deleted. However, since *E. coli* KJ 122 does have a full TCA cycle, it is able to produce additional NADH by producing SA through the oxidative branch of the TCA cycle. This difference can be easily seen in Figure 2-2.

E. coli KJ 122 also contains a complete glyoxylate cycle, which can be used in a similar fashion to produce NADH, and results in exactly the same net equation and therefore the same yields, although this is mostly active under aerobic conditions. Since the genes that produce acetic acid, lactic acid and formic acid have been removed, this can theoretically be done without any byproducts forming. The maximum theoretical yield for *E. coli* KJ 122 is therefore exactly the same as the stoichiometric maximum yield (1.12 g/g). This yield is calculated by assuming that only the pyruvate dehydrogenase pathway is active in converting pyruvate to acetyl-CoA.

Jantama *et al*. (2008) were able to obtain an SA yield of 0.96 g/g during batch fermentations using *E. coli* KJ 122, almost 86% of the theoretical SA yield.

Table 2-1: The relevant gene modifications made to *E. coli* C to obtain the succinate-producing *E. coli* KJ 122 (Jantama *et al*., 2008; Van Heerden & Nicol, 2013)

Enzyme	Modification	Abbreviation
2-ketobutyrate formate lyase	Inactivation	ΔtdcE
Acetate kinase	Inactivation	ΔackA
Alcohol dehydrogenase	Inactivation	ΔadhE
Aspartate aminotransferase	Inactivation	ΔaspC
Citrate lyase	Inactivation	ΔcitF
Formate transporter	Inactivation	ΔfocA
Lactate dehydrogenase	Inactivation	ΔldhA
Methylglyoxal synthase	Inactivation	ΔmgsA
NAD+-linked malic enzyme	Inactivation	ΔsfcA
PEP carboxikinase	Overexpression	Δpck
Pyruvate formate lyase	Inactivation	ΔpflB
Pyruvate oxidase	Inactivation	ΔpoxB
Threonine decarboxylase	Inactivation	ΔtdcD

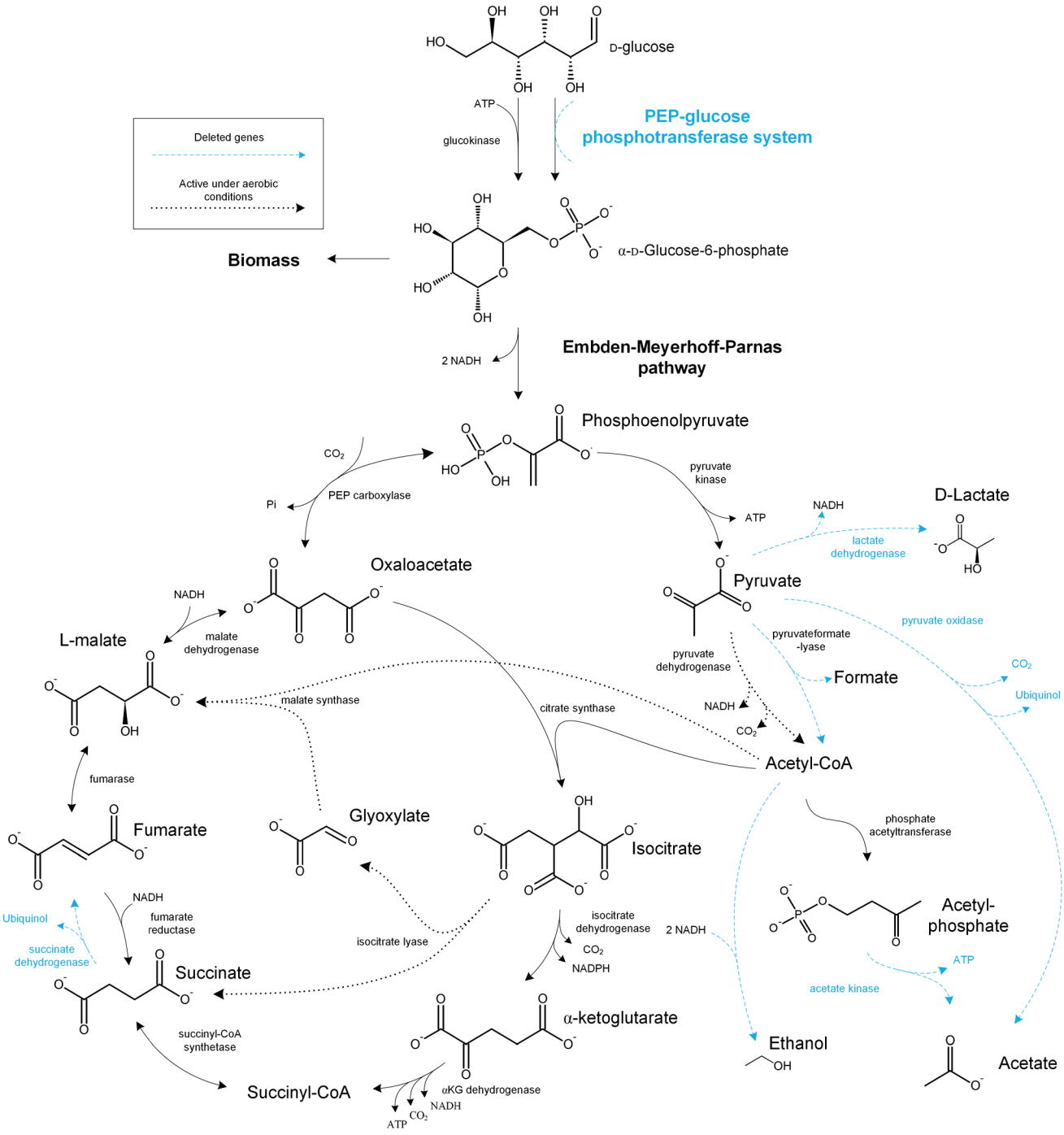

Figure 2-3: Standard pathway for the metabolism of glucose in *E. coli* (Jantama *et al*., 2008; Van Heerden & Nicol, 2013)

Solid arrows represent enzymatic reactions that are expected to be active under anaerobic conditions. Dotted arrows represent enzymatic reactions that function mainly under aerobic conditions. Blue dashed arrows represent genes that have been eliminated in *E. coli* KJ 122

Jantama *et al*. (2008) did, however, find that pyruvate formed a byproduct. This was attributed to an overflow from glycolysis, and was reduced during fermentations at lower sugar concentrations. The high pyruvate concentrations might promote the overproduction of acetyl~CoA, which in turn could lead to the formation of acetic acid. Although all pathways leading to acetate had been removed, significant amounts of acetate were still formed during fermentations. A possible explanation is that acetyl~P is converted to acetate by unspecified reactions, which could include the phosphorylation and dephosphorylation of proteins, spontaneous hydrolysis, and other reactions (Jantama *et al*., 2008).

Formate was detected during fermentations, suggesting some pyruvateformate-lyase activity, although the gene was inactivated. The formate concentrations did, however, decrease to trace amounts during late stages of batch fermentations, most probably converted to H_2 and CO_2 by formate dehydrogenase. Much as in the naturally producing bacteria, the maximum theoretical yield for *E. coli* KJ 122 is, however, lower if the pyruvateformate-lyase pathway is active, since NADH is not formed due to the formation of formic acid. Equation 2 shows the net reaction if only the pyruvateformate-lyase pathway is active, resulting in a theoretical yield of 1.09 g/g. Nevertheless, this yield is still higher than that obtained with bacteria that naturally produce SA.

$$Gluc + CO_2 \rightarrow \frac{5}{3}SA + \frac{1}{3}FA + \frac{2}{3}H_2O \quad (2)$$

2.4 Cell recycling

Cell perfusion or recycling is the continuous process whereby medium is continuously supplied to the bioreactor, the cells from the spent culture medium are continuously separated and returned to the reactor, while the rest of the spent culture medium is harvested. Perfusion is not a new technique, and was already applied in 1912 to keep small tissue samples viable (Schügerl & Zeng, 2007:133).

In a batch process the cells are subjected to a constantly changing environment, which limits the potential for growth and metabolic expression. This can be overcome to some extent by fed-batch strategies, by which higher cell concentrations can be

achieved by constantly adding new medium to the reactor. Any toxic byproducts produced will, however, accumulate in the reactor, limiting the operation time.

In continuous cell recycle cultures, exchange of the in situ medium allows extremely high cell concentrations (due to the constant removal of products, which may be toxic) and the constant supply of fresh nutrients. The reactor also operates at steady state, allowing far better control of the reactor operating conditions (pH, dissolved oxygen levels, substrate and product concentrations). The high cell concentrations usually allow high product titres, even at high dilution rates, resulting in significantly higher productivities. This allows the use of smaller reactors, with high throughput, reducing the capital costs. Furthermore, when compared with batch and semi-batch cultures, the unproductive growth phase is a far smaller portion of the total fermentation time. Oxygen transfer can, however, become a significant problem for aerobic organisms at high cell concentrations (Schügerl & Zeng, 2007:131–133).

The effectiveness of the cell retention devices used for recirculation is an extremely important design consideration. The device should have a high cell retention efficiency and be capable of long-term operation without considerable fouling. It is also essential that the device is cleanable and sterilisable, either chemically or through heat sterilisation. For large-scale operations, long-term reusability is also essential, although many laboratory-scale operations use disposable products (Schugerl & Zeng, 2007:134).

Many different devices have been used for cell separation. Those most commonly used include:

- Centrifuges and hydrocyclones
- Settling of flocculent microorganisms
- Membrane separation, including:
  - Cross-flow filtration
  - Dead-end filtration

In membrane devices extremely high cell densities are possible because, unlike with the other methods, complete recycling of the cells in the reactor medium is possible. Membrane fouling does, however, occur after a certain operation time (especially in

dead-end filtration), although steps can be taken to decrease fouling rates (Van Reis & Zydney, 2007).

2.4.1 Membrane devices

Various membrane devices have been successfully used for cell recycling, each with specific advantages and drawbacks, including:

- Internal devices (such as spin filters and submerged membranes)
- Flat sheet filters
- Spiral-wound membranes
- Hollow fibre filters (HFF)

An HFF was chosen for this study due to ease of sterilisation, effective minimisation of fouling, ease of installation and operation, and the simplicity of scaling up the system. Accordingly, the rest of the discussion will focus on filters of this type.

HFF modules consist of a bundle of thin tubular membranes, with inner diameters from 0.2 to 1.8 mm. Each module can contain between 50 and 3 000 individual fibres. The membrane fibres can be made from various polymers, depending on the application. The bundles are placed in a housing, in a shell-and-tube configuration, and bound at each end with epoxy. The fibres typically have an asymmetrical membrane, with a thin, dense skin on the inside. The fibres are self-supporting and typically can be cleaned with backwashing techniques. The feed is pumped through the bore of the fibres and the permeate is collected from the shell side. HFF modules typically come in short lengths, 18-100 cm, to reduce the pressure drop across the module, and because shorter lengths tend to lead to higher flux due to mass transfer effects.

Most fibres have low pressure ratings – the maximum transmembrane pressure (TMP) is usually 1–3 bar. High-pressure operation is therefore not possible and the pressure drop across the module has to be kept below these ratings. HFFs typically operate in the laminar flow region, with velocities of 0.5–2.5 m/s. The combination of high velocity and small tube diameters leads to high shear rates (2 000-16 000 s^{-1}). The modules are, however, susceptible to blockages at the inlet due to the small tube diameters (Cheryan, 1998:190–201).

2.4.2 Filter system design criteria

At high cell concentrations, membrane fouling can become quite severe, and it is therefore one of the largest limitations to long-term fermentation. The filter criteria are therefore specified to limit fouling as much as possible.

Membrane fouling is considered an “irreversible” process, causing a decline in flux for constant-pressure operations. Fouling is caused by the build-up of components on the membrane surface and/or in the pores of the membrane, which is a result of interactions between the membrane and solutes in the feed. Fouling increases the capital costs due to the decline in flux, and restoring the flux of the membrane might require harsh cleaning methods, which reduce the lifespan of the membrane (Cheryan, 1998:245–255).

Because membrane fouling is caused by a complex interaction between the membrane and various solutes, it is extremely difficult to create general rules to limit fouling.

Inherent aspects of the membrane (such as hydrophilicity, membrane surfaces, membrane charge and pore size) can contribute significantly to the rate and severity of fouling (Cheryan, 1998:245–255). The solutes or suspended particles being separated have just as significant an impact on fouling as the membrane itself, and particles such as proteins, salts and fats are a major source of fouling (Cheryan, 1998:256–263).

A final aspect that could affect fouling, and also the simplest to control, is the process parameters at which the filter is operated and the parameters of the membrane itself (Cheryan, 1998:263–266).

Recirculation rate: High shear rates usually shear off particles deposited on the membrane surface, increasing flux. However, at high velocities the shear-induced lift of larger particles becomes significant, thus lifting them clear of the membrane surface. This could cause a layer of smaller particles to form on the membrane surface, exacerbating the fouling at higher shear rates.

Transmembrane pressure: At low pressures, the flux increases as the pressure increases, but at higher pressures the flux becomes a function of mass transfer due to a concentration polarisation layer, and a further increase in pressure will only

increase the flux momentarily. As fouling layers form, they become compressed at higher pressures, leading to lower flux at higher pressures.

Membrane area: The membrane flux required understandably decreases as the membrane area increases, thereby lowering the rate of fouling. The optimal area does, however, depend on the membrane cost and lifespan, as well as the cost of recycling the medium through the filter.

Pore size: When selecting a pore size, the relative size of the solutes is very important. If the pore size is of the same order of magnitude as that of the separated particles, some particles could become lodged in the pores, blocking them physically. This leads to a rapid initial decline in flux, since it is usually the larger pores that are blocked first. Cheryan (1998:254) suggests a ratio of particle to pore size of 10. Pore sizes that are too small will, however, lead to other membrane-related factors that limit the flux. There is therefore usually a pore size that would offer the optimal average flux.

3 Experimental

3.1 Microorganisms and inoculums

A modified strain of *E. coli* (KJ 122) was acquired from the Department of Microbiology and Cell Science of the University of Florida, USA, and used for all fermentations. The culture stock was stored in a 66% glycerol solution at -20 °C. Inoculums were incubated at 37 °C and 100 r/min for 16–24 h in 50 mL Schott screw-capped bottles containing 30 mL of sterilised Luria-Bertani broth (LBB). Each inoculum was prepared from frozen stock cultures to avoid mutation.

The inoculums were analysed by high-performance liquid chromatography (HPLC) to test the purity of the inoculum. The inoculum was deemed infected if lactic acid or ethanol was detected.

3.2 Fermentation medium

Unless specified otherwise, all chemicals used in the fermentations were obtained from Merck KgaA (Darmstadt, Germany). A defined medium (AM1), developed by Martinez *et al*. (2007), was used in all the fermentations. A concentrated stock solution of the trace metals was made by dissolving 1 000 times the required amount of metals in a 120 mM HCl solution. The medium was supplemented with 50 g/L D glucose for continuous fermentations and 90 to 100 g/L D-glucose for batch fermentations, as the carbon source. Antifoam Y30, 0.5–1 g/L (Sigma–Aldrich, St. Louis, USA) was also added to prevent foaming. Additional antifoam was pumped directly into the reactor as needed. CO_2 gas (Afrox, Johannesburg, South Africa) was fed into the reactor as an inorganic carbon source, at a flow rate of 10% vvm. The medium composition is given in Table 3-1.

Table 3-1: *E. coli* AM1 defined fermentation medium composition, with concentrated salt solution composition

Component	Concentration [g/l]	Source
Main medium components		
$(NH_4)_2HPO_4$	2.6308	Merck KgaA
$NH_4H_2PO_4$	0.8696	Merck KgaA
KCl	0.1491	Merck KgaA
$MgSO_4$	0.1805	Merck KgaA
Betaine	0.0187	Sigma-Aldrich
Glucose-H_2O	55	Merck KgaA
Concentrated trace metal solution	1 mL/L	
Concentrated trace metal solution (1 000x)		
HCl	4.3741	Merck KgaA
$FeCl_3$-$6H_2O$	2.4002	Merck KgaA
$CoCl_2$-$6H_2O$	0.2998	Merck KgaA
$CuCl_2$-$2H_2O$	0.1500	Merck KgaA
$ZnCl_2$	0.2999	Merck KgaA
Na_2MoO_4-$2H_2O$	0.3000	Merck KgaA
H_3BO_3	0.0748	Merck KgaA
$MnCl_2$-$4H_2O$	0.4948	Merck KgaA

3.3 Bioreactor

A Jupiter 2.0 (Solaris biotechnology, Italy) autoclavable fermentation system was used, which was composed of a 1.5 L jacketed fermentation vessel, a touch screen PC with Leonardo control software installed and a control module.

A simplified schematic of the reactor setup during batch runs can be seen in Figure 3-1.

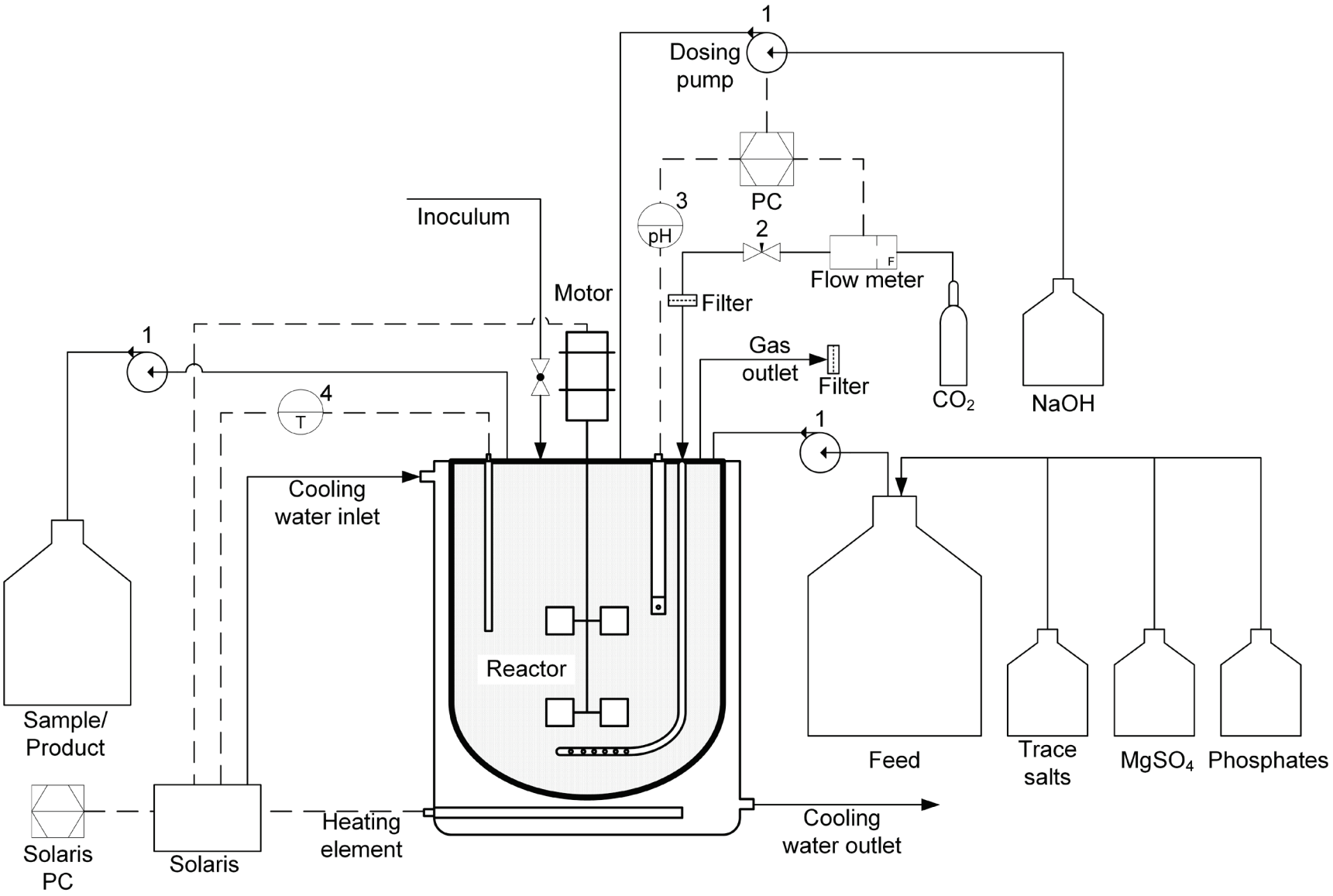

Figure 3-1: Schematic of the reactor setup for batch fermentations. The numbered symbols are: 1: peristaltic pumps, 2: needle valve, 3: pH control system and 4: temperature data line

The reactor is equipped with:

- A removable motor, connected to a sealed agitation shaft
- An agitation shaft equipped with two Rushton turbine impellers
- A pH probe, thermocouple, dissolved oxygen sensor and an anti-foam sensor
- A gas sparger
- 14 threaded holes used for the various probes and reactor inlets/outlets (sealed with O-rings)
- A glass jacket with two heating elements and cooling water for temperature control

The control module connects directly to the PC, through a USB connection.

The control module contains:

- Four Watson & Marlow peristaltic pumps
- An electric water valve, to control the flow of cooling water to the reactor jacket
- A mass flow meter and electric valve, to control air flow into the reactor (not used)
- Connections for the thermocouple, pH probe, DO probe, heating elements, anti-foam sensor and motor

The standard Jupiter system has excellent temperature control and adequate pH control. The integrated data acquisition program does, however, only record data every minute, and does not record the pump speed of the base flow. The volume of NaOH/KOH added to the reactor could therefore not be determined with the system.

The system was therefore equipped with a separate pH controller (Liquiline, Endress & Hauser) and pH probe, with a temperature sensor (ISFET Sensor CPS471D, Endress & Hauser).

Since the gas flow system in the control module was calibrated for air, a Brooks mass flow controller was used to control CO_2 flow rates.

A cDAQ-9184 (with NI 9265 & NI 9207 modules; National Instruments) was used to link the mass flow controller, pH controller and pump to a computer. A customised LabView (National Instruments) program was written to monitor the reactor and record the data in an Excel file.

The pH was controlled at a set-point of 7. To achieve pH control, an NaOH/KOH dosing pump was connected to a relay in the Liquiline pH controller. The controller switched the

relay, and in turn the pump, on when the pH dropped below 7 and switched it off again when the pH was equal to, or greater than, 7. The cDAQ read the voltage across the relay; if this value is multiplied by the pump flow rate and then time averaged in LabView, the average dosing flow rate can be estimated. The average dosing flow rate can be used to estimate the SA productivity in the reactor, without the need for physical analysis.

The cDAQ also received (in a 4–20 mA signal) the measured flow rate from the mass flow controller and the measured temperature and pH from the pH probe. The 4–20 mA signal is then converted to the relevant units in LabView, and recorded.

3.3.1 Membrane criteria selection and cell recycle operation

The important criteria of the filtration system (namely membrane area, pore size, recirculation rate and transmembrane pressure) were selected based on previous cell recycle studies (see Table 3-2). The HFF selected had a polysulphone membrane with a total membrane area of 1 200 cm^2 and a 500 000 nominal molecular weight cut-off (NMWC) pore size (UFP-500E-5A, GE Healthcare, Westborough, UK).

The membrane area was chosen based mostly on the membrane flux, although a general value of membrane area per volume of reactor, s/v, was also used. Flux values ranged from 0.49 to 17.14 L/m^2h. A higher flux did, however, tend to lead to shorter fermentation times and, in some cases, fouling. Most of the longer fermentation times were achieved below a flux of 4.5 L/m^2h. A maximum flux of under 2 L/m^2h was therefore chosen as a suitable value. The membrane area is given per volume of reactor in order to compare the values. A large range of s/v values (0.05 to 12 cm^{-1}) was observed, with most of the values being between 0.4 and 4.25 cm^{-1}.

A membrane area of 1 200 cm^2 would result in a maximum flux of 1.7 L/m^2h and an s/v value of 0.8 cm^{-1}. The relatively low s/v value was deemed appropriate since the reactor would be operated at lower dilution rates than those of the studies in Table 3-2.

A remarkably large range of recirculation rates per membrane area (r/s) was observed in cell recycle studies (5.4 to 320 cm/h for HFFs). The r/s is not the ideal variable to compare membrane performance; the shear rate at the membrane surface would be more appropriate since it does not depend on the membrane geometry. Most articles do not, however, state the shear rate and far too few values were available to calculate the shear rate. At a constant r/s the shear rate will, for example, be higher in an HFF with smaller fibre

diameters. A recirculation rate of around 2 L/h was used, resulting in an r/s value of 1.6 cm/h, although this could be changed by simply modifying the pump speed.

Polysulphone (PS) membranes are significantly more common than any other material. Polypropylene (PP) and cellulose tri-acetate (CTA) were each used in only one of the papers referred to (Nolasco-Hipolito & Matsunaka, 2002; Zeng, Biebl & Deckwer, 1991). Most HFF devices used PS membranes, although, because of the complex solute-membrane interaction, the membrane materials chosen cannot be easily compared. The effectiveness of the membrane material will depend on the nature of the feed used and the operating conditions required. PS can, however, handle relatively high temperatures, and can therefore be sterilised in an autoclave. It was therefore chosen as the preferred material.

To operate the reactor continuously with cell recycle, only a few modifications were made. The inlet and outlet of the autoclavable HFF were connected to the reactor, with a high-volume peristaltic pump to recirculate the medium. Two pressure gauges were placed on the filter, one at the inlet and one on the permeate side of the filter, to calculate the trans-membrane pressure and ensure that the inlet pressure did not exceed the maximum pressure rating. A pump was placed on the permeate line to control the permeate flow rate and to supply a back pressure to the filter, reducing fouling. A simplified version of Figure 3-1 equipped with cell recycle equipment is given in Figure 3-2.

Table 3-2: Summary of previous continuous cell recycle studies using hollow fibre filters

Reference & strain	Product	Pore size[b] [µm; MW]	Material	D_t [*c] [h^{-1}]	Bleed [h^{-1}]	Biomass [g/l; OD_{600}]	Productivity [g/L/h]	s/v[*d] [cm^{-1}]	r/s[*e] [cm/h]	Flux [L/m^2h]	MFT [*f] [h]	Fouling[*a]
Borch, Berg & Holst, 1991; *Lactobacillus*	Lactic acid	1 000 k	n/a	0.55	0	3.1 x 10^{10} cells/ml	3.8	1.40	8.6	3.93	87	N
Cheryan & Mehaia, 1983; *Kluyveromyces fragilis*	Ethanol	50 k	PS	6.00	0	90	240	3.50	n/a	17.14	24	Y
				1.00	0	90	75	3.50	n/a	2.86	24	Y
Jang, Malaviya & Lee, 2013; *Clostridium acetobutylicum*	ABE	n/a	n/a	0.9	0.04	335 [OD_{600}]	21.1	12.00	n/a	0.75	935	N
			n/a	0.9	0	407 [OD_{600}]	19.3	12.00	n/a	0.75	935	N
Kim, 2009; *Actinobacillus succinogenes*	Succinic acid	300 k	n/a	0.2	0.01	16.4	3.71	0.40	36	5.00	40	Y
				0.3	0.01	13.5	4.5	0.40	36	7.50	40	Y
				0.4	0.02	13	6.25	0.40	36	10.00	25	Y
				0.5	0.02	13.1	6.63	0.40	36	12.50	40	Y
Mannheimia succinici-producens		300 k	n/a	0.1	n/a	7	1.28	0.40	36	2.50	85	N
Lee *et al.*, 1998; *Halobacterium halobium*	Bacterio-rhodopsin	500 k	PS	0.1	0	30.3	0.0012	0.43	110.8	2.31	245	N
Lee, Gu & Chang, 1989; *Escherichia coli*	Tryptophan	50 k	n/a	0.23	0	19.76	2.07	0.43	n/a	5.31	48	Y
				0.39	0	31.2	3.9	0.43	n/a	9.00	48	Y
Nolasco-Hipolito & Matsunaka, 2002; *Lactococcus zactis*	Lactic acid	0.1	CTA	0.21	0.04	4.6	8.2	4.25	n/a	0.49	500	N
				0.44	0.11	5	16.2	4.25	n/a	1.04	500	N
				0.5	0.11	6	19.3	4.25	n/a	1.18	500	N
				0.75	0.13	10	27.6	4.25	n/a	1.76	500	N

Reference & strain	Product	Pore size*b [µm; MW]	Material	D_t *c [h^{-1}]	Bleed [h^{-1}]	Biomass [g/l; OD_{600}]	Productivity [g/L/h]	s/v*d [cm^{-1}]	r/s*e [cm/h]	Flux [L/m^2h]	MFT *f [h]	Fouling*a
Park, Ohtake & Toda, 1989; *Acetobacter aceti*	Acetic acid	0.1	n/a	0.3	0	22.5	12.7	3.33	13.5	0.90	830	N
Pierrot, Fick & Engasser, 1986; *Clostridium acetobutylicum*	ABE	100 k	PS	0.3	0.027	20	4.5	0.28	57.8	10.91	200	N
Tashiro *et al*., 2005; *Clostridium saccharoperbutyl -acetonicum*	ABE	0.1	PS	0.765	0.09	32.7	8.82	4.25	n/a	1.80	207	N
				0.85	0.09	33.1	9.77	4.25	n/a	2.00	60	N
				0.85	0.11	21.7	6.62	4.25	n/a	2.00	207	N
				0.85	0.14	17.2	8.2	4.25	n/a	2.00	207	N
Yoo *et al*., 1997; *Lactobacillus casei*	Lactic acid	100 k	PS	0.11	0.054	11.1	3.51	1.03	96.9	1.07	130	N
				0.11	0.023	27.9	3.36	1.03	96.9	1.07	130	N
				0.23	0.051	87	12	1.03	96.9	2.23	130	N
Zeng, Biebl & Deckwer, 1991; *Enterobacter aerogenes*	2,3-butanediol	0.2	PP	0.23	0.015	56.6	12.51	0.40	320.6	5.75	170	N
				0.25	0.015	56.7	13.03	0.40	320.6	6.25	170	N
				0.27	0.015	62.2	14.64	0.40	320.6	6.75	170	N

n/a: Information not available
*a "Y" if fouling or anti-fouling methods were discussed
*b MW: Pore sizes with molecular weight cut-off values are given as ## k, implying ##x1 000
*c D_t: Total dilution rate
*d s/v: Surface area per reactor volume
*e r/s: Recirculation rate per surface area
*f MFT: Maximum fermentation time

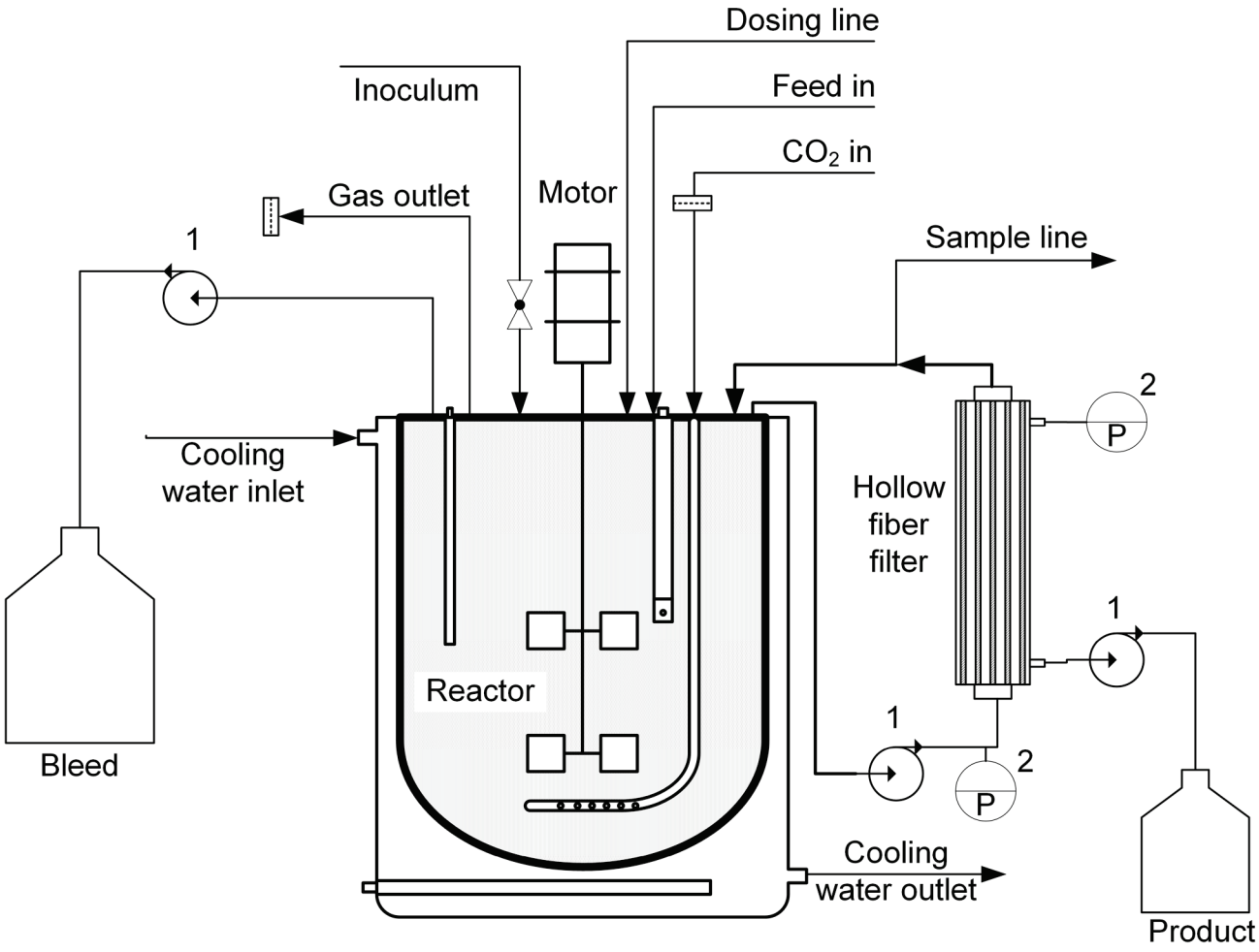

Figure 3-2: Reactor equipped for cell recycling. The same control system as in Figure 3-1 was used. The numbered symbols are: 1: peristaltic pumps and 2: autoclavable pressure gauges

3.4 Fermentation

For both the continuous and batch fermentations the reactor, tubes, medium reservoirs and HFF for continuous cell recycle fermentations were autoclaved together for 40 min at 125 °C. A bottle was placed on the feed sample line, and another on the reactor sample/product line, to ensure a closed system. To prevent precipitation and unwanted reactions of salts in the medium, the glucose, trace salts (with KCl and betaine), phosphates and $MgSO_4$ were all separated during autoclaving and mixed after the solutions had cooled. The KOH reservoir was also

connected to the reactor, but was kept empty and filled with 10 M KOH after the reactor had cooled.

The reactor was filled with 1.3–1.5 L of medium and CO_2 flow was established, to maintain a positive pressure in the reactor. The temperature control of the reactor was set to 37 °C and the agitator at low r/min. The reactor was then left for 24 h, after which the reactor and medium reservoir were sampled to check for infection.

After 24 h the CO_2 flow was adjusted to about 0.1 vvm (10% of the reactor volume per minute). Once the temperature and pH had stabilised, and sterility had been confirmed through HPLC analysis, 20 ml of inoculum was injected into the reactor through a rubber septum in the head of the reactor. The temperature and pH were maintained at 37 °C and 7 respectively, with the stirring speed set to 400 r/min. Batch runs were continued until the succinic acid production rate was negligible (approximately 5 days), with samples taken at regular intervals to determine substrate and product concentrations. For continuous fermentations, the reactor was first operated in batch fashion to build up sufficient biomass, and the dilution rate was then set to the required rate. The dilution rate was varied from 0.05 to 0.15 h^{-1}.

3.5 Analytical methods

All product and substrate concentrations were determined using HPLC and cell concentrations were determined by using the dry cell weight (DCW) of samples.

3.5.1 High-performance liquid chromatography (HPLC)

An Agilent 1260 Infinity HPLC (Agilent Technologies, USA) was used to determine the glucose, ethanol and organic acid concentrations. The HPLC was equipped with a refractive index detector and a 300 x 7.8 mm Aminex HPX-87H column (Bio-Rad Laboratories, USA). A 0.3 ml/L H_2SO_4 solution was used as the mobile phase, at a column temperature of 60 °C.

A 20 mL sample was taken from the bioreactor (for HPLC analysis and DCW calculation), and centrifuged for 90 s at 17 000 r/min. The supernatant fluid was filtered using a 0.2 µm filter, and 500 µL of the filtered sample was then transferred to a HPLC sampling vial and diluted with 1 000 µL of filtered, distilled water.

3.5.2 Dry cell weight (DCW)

The DCW was determined from 18 mL samples centrifuged at 12 100 g for 90 s. The supernatant was drained. The cell pellet was washed twice with distilled water, and centrifuged between washes. Distilled water was then used to re-suspend the solids into a dry, weighed vial, using a pipette. The vial was dried in an oven for at least 24 h at 85 °C, and weighed again to determine the mass of solids. Since it took 24 h to analyse the DCW samples, the DCW was estimated by measuring the optical density (OD) of the re-suspended biomass using a spectrophotometer. The OD per DCW did not, however, remain constant throughout a run, and the DCW was therefore seen as a more accurate representation of the biomass in the reactor.

Small biomass concentration measurements (DCW < 0.4 g/L) were regarded as inaccurate due to unavoidable errors in the weighing of the vials.

3.6 Data analysis

3.6.1 Batch analysis protocol

In order to account for the volume increase due to the KOH dosing, and the volume decrease due to sampling, all the batch data are calculated in grams produced rather than concentration. To compare the data with those from continuous runs, they were then divided by the initial batch volume, 1.5 L, to obtain a concentration. This should not affect the data significantly since the batch volume stayed very close to the initial volume throughout the fermentation, with the KOH dosing replacing the volume of the samples removed. However, since the samples needed to be large enough to calculate the DCW, a significant amount of metabolite and glucose was removed with the samples. It was therefore necessary to account for the substrate and metabolites removed.

The volume at each sample point was calculated by using Equation 3 and the concentration of metabolite (SA, AA and glucose) produced (C_i^*) was then calculated using Equation 4. The accumulated volume of KOH (AccKOH) at the time of sampling was used each time. The amount removed with the samples of metabolites that decrease later in the batch (formic acid (FA), pyruvic acid and DCW) was not accounted for since this skews the data on the metabolites, resulting in values far above the actual amounts left in the reactor. Fortunately, the amount of these

metabolites that were removed is far smaller than that of the other metabolites, due to the drastic decrease in concentration later in the fermentation, at which stage a number of samples were taken. These metabolites were therefore calculated using Equation 5.

$$V = V_{t=0} + AccKOH_{t=i} - \sum_{s=1}^{i}(V_{sample}) \tag{3}$$

$$C_i^* = \frac{1}{V_{t=0}}\left[C_i V + \sum_{s=1}^{i}(C_{i,sample}V_{sample})\right] - C_{i,t=0} \tag{4}$$

$$C_i^* = \frac{(C_i V - C_{i,t=0}V_{t=0})}{V_{t=0}} \tag{5}$$

3.6.2 Definition of steady state

To determine whether a sample was taken at a reasonably steady state two methods were used in unison. First an average of the measured KOH dosing flow rate was calculated from 10 hours before each sample time. If the measured KOH dosing flow rate was within 10% of the average dosing flow rate, then steady state was initially assumed. Secondly the HPLC results were compared to other points at similar conditions, if the sample was significantly different, it was assumed that the point was not at steady state, even if the dosing flow rate was steady.

3.6.3 Metabolic flux analysis

Metabolic flux can be expressed as the rate of carbon flow through a specific metabolic pathway. The flow of carbon through these metabolic pathways can be analysed by flux analysis. The fluxes are calculated at steady state, using the net rate production of products and substrates, since these are the only fluxes that can be measured directly. However, to calculate the internal fluxes, further constraints are necessary. These constraints can be imposed on the flux network by (Nielsen, Villadsen & Lidén, 2011:155):

- A total carbon balance, where the carbon fed to the flux network is equal to that leaving the network
- An NADH balance where the redox consumed and produced should be equal
- The stoichiometric relationship between internal fluxes

A simplified version of the metabolic pathways of *E. coli* KJ 122, seen in Figure 3-3, was used for the flux analysis. The pathways were further simplified by removing the pathways that are mostly active under aerobic conditions. The glyoxylate shunt was therefore not considered in the metabolic flux analysis since it is mostly active only under aerobic conditions. Certain pathways that should be inactive, such as the pyruvateformate-lyase pathway, were added since evidence of the pathway was detected (in this case by the formation of formate).

Once the needed constraints had been imposed, the unknown flux values were solved at each steady state sample. This was done by using the numerical programming language Octave to solve the matrix-based description of the metabolic network. (Nielsen, Villadsen & Lidén, 2011:166)

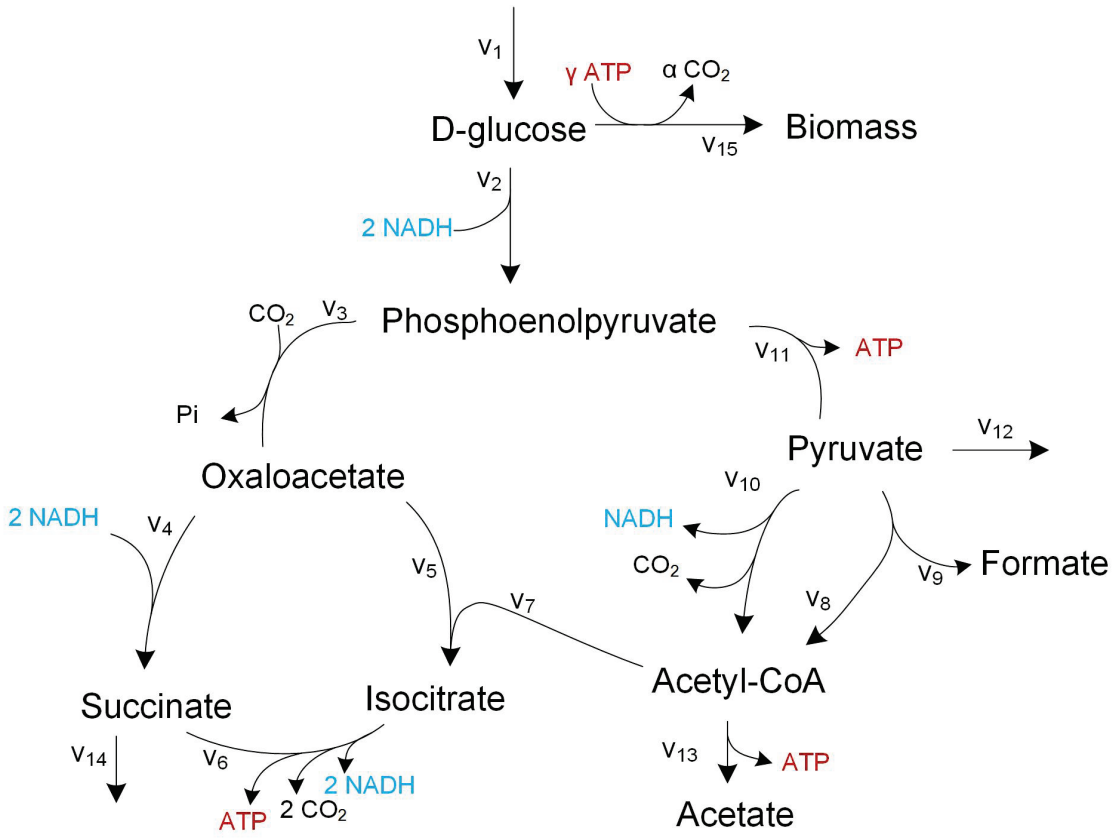

Figure 3-3: Simplified metabolic pathways for the anaerobic metabolism of glucose in *E. coli* based on the more complete pathways in Figure 2-3

Each of the fluxes in the metabolic flux analysis were numbered, as indicated by Figure 3-3. Most of the important values from the flux analysis can be represented through the ratio of various fluxes. These include the following:

- The fraction of PEP converted to pyruvate instead of oxaloacetate, represented by PEP_{pyr} in Equation 6
- The fraction of acetyl-CoA converted to isocitrate instead of acetate, represented by $ACoA_{cit}$ in Equation 7
- The fraction of pyruvate converted to acetyl-CoA through pyruvate dehydrogenase instead of through pyruvateformate-lyase, represented by Pyr_{pdh} in Equation 8
- The fraction of pyruvate excreted instead of converted to acetyl-CoA through pyruvate dehydrogenase or pyruvateformate-lyase, represented by Pyr_{out} in Equation 9

$$PEP_{pyr} = v_{11}/v_2 \tag{6}$$

$$ACoA_{cit} = v_7/(v_7 + v_{13}) \tag{7}$$

$$Pyr_{pdh} = v_{10}/(v_{10} + v_9 + v_8) \tag{8}$$

$$Pyr_{out} = v_{12}/v_{11} \tag{9}$$

Equation 6 (PEP_{pyr}) shows the fraction of the carbon flux that enters the oxidative branch of the TCA cycle instead of the reductive branch. This is important since the oxidative branch of the TCA cycle is responsible for the formation of byproducts, as well as the formation of additional NADH which can be used to form SA in the reductive branch of the TCA cycle.

The values from Equations 7, 8 and 9 were deemed important since they represent the production of unwanted byproducts.

The value of Pyr_{pdh} is also important since the additional NADH produced through pyruvate dehydrogenase can be used in the reductive branch of the TCA cycle, thus increasing the yield of SA.

3.6.4 Mass balance

In order to assess the accuracy of the samples, a mass balance was performed on each sample. By calculating the glucose needed to form the metabolic products, it was possible to compare this value with the amount of glucose consumed, obtained experimentally. A term “closure” was then defined as the calculated glucose divided by the experimental glucose consumed.

The stoichiometric value of glucose needed to form the metabolic products was determined using an elemental “black box” stoichiometric model (Nielsen, Villadsen & Lidén, 2011:96). Due to dilution effects from the KOH dosing, the initial glucose was calculated using Equation 10. The experimental glucose consumed was then simply calculated by subtracting the glucose in the reactor from the initial glucose.

$$C_{GLe} = C_{GL0}\left(\frac{Q_{feed}}{Q_{feed} + Q_{KOH}}\right) \tag{10}$$

4 Results and discussion

4.1 Batch fermentation results

Three batch fermentations were undertaken during the study. All batch fermentations were performed with an initial volume of 1.5 L and an initial glucose concentration of 90 to 102 g/L. The details of the batch fermentations are given Table 4-1. Apart from Batch 2, the fermentations were performed until the SA production rate was negligible, which occurred well before all the glucose had been consumed, with more than 20 g/L of glucose being left in the reactor after production had stopped. Batch 2 was terminated prematurely due to a CO_2 shortage.

The repeatability for all three batch runs was extremely good, as seen in the SA and AA concentrations of the three runs in Figure 4-1. As can be seen in Figure 4-1 and Figure 4-2, the concentration of DCW, pyruvate and formate decreased significantly as the fermentation progressed. Batch 2 did not, however, show the full extent of the decrease since it was terminated prematurely.

To ensure that none of the unmeasured substrates in the AM1 medium were depleted during the fermentations, causing a drop in productivity and cell growth, one fermentation had to be done with more of the unmeasured substrates. Batch 3 was therefore done using 1.5 times the concentration of all the medium components given in Table 3-1. As seen in Figure 4-1, this did not influence the SA or biomass concentrations. It was therefore assumed that no substrate depletion occurred.

Table 4-1: Differences in batch fermentations performed

Batch number	Glucose t = 0 [g/L]	Medium salt concentration
1	90.9	Standard AM1 medium
2	102.3	Standard AM1 medium
3	100.5	AM1 medium with 1.5 times the concentration of all components

The final concentration of SA and AA produced, as well as the glucose consumed, during the batch fermentations can be seen in Table 4-2. The SA and AA overall yields are also given in the table, with the maximum SA yield being 0.85 g/g.

Table 4-2: Final concentration of metabolites produced during batch fermentations, with the resulting yields

Batch number	Glucose consumed [g/L]	SA produced [g/L]	AA produced [g/L]	Y_{SP} [g/g]	Y_{SA} [g/g]
1	70.0	59.2	10.5	0,85	0,15
2	60.4	46.2	7.4	0,77	0,12
3	69.7	59.1	9.7	0,85	0,14

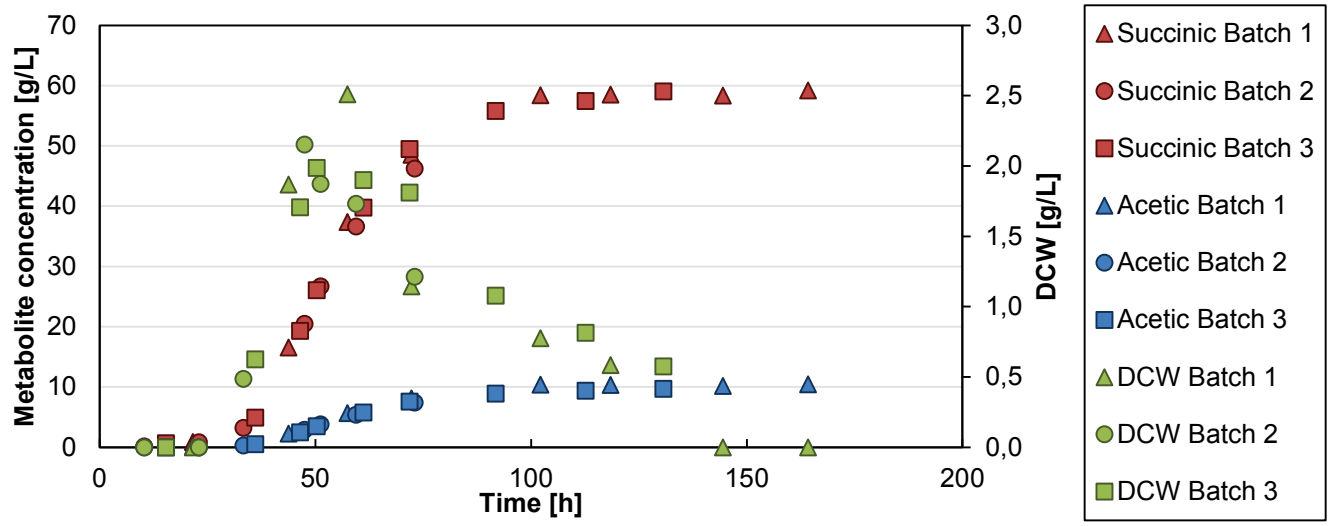

Figure 4-1: Concentration profiles of three separate batch runs, showing the repeatability of the runs

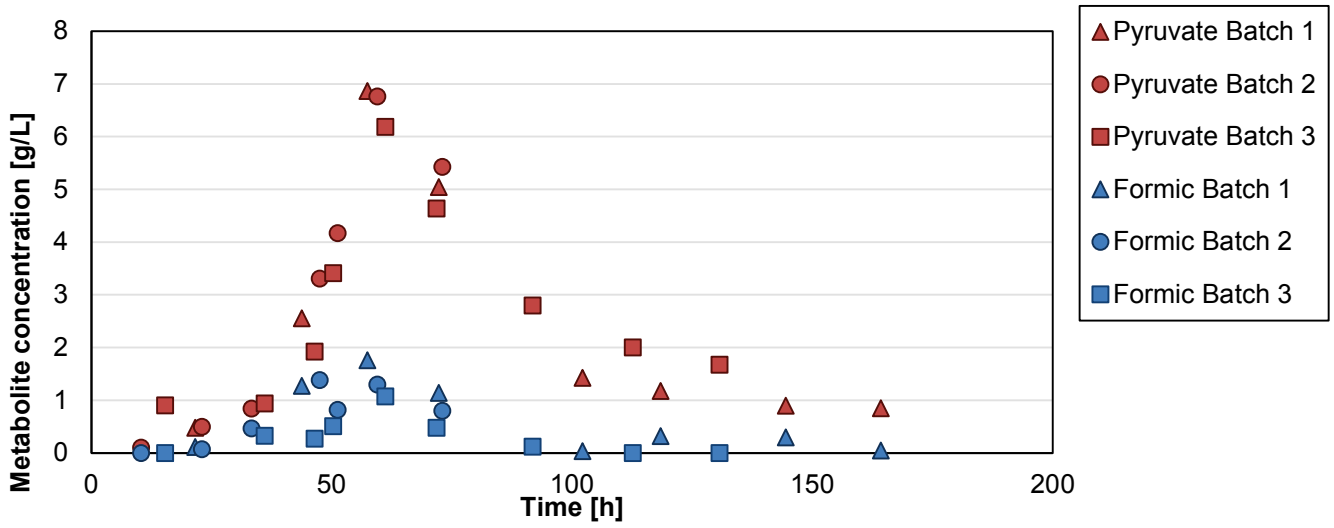

Figure 4-2: Concentration profiles of the byproducts pyruvate and formate, showing the decrease in concentration as the fermentation proceeds

The SA productivity throughout the batch fermentations was estimated by calculating the slope between the sample points, and then using the average time of the two samples (Figure 4-3). In order to be able to compare the batch productivity data with those of continuous runs, the productivity was then divided by the initial batch volume, 1.5 L. This should not affect the data significantly since the batch volume stayed very close to the initial volume throughout the fermentation, with the KOH dosing replacing the volume of the samples removed.

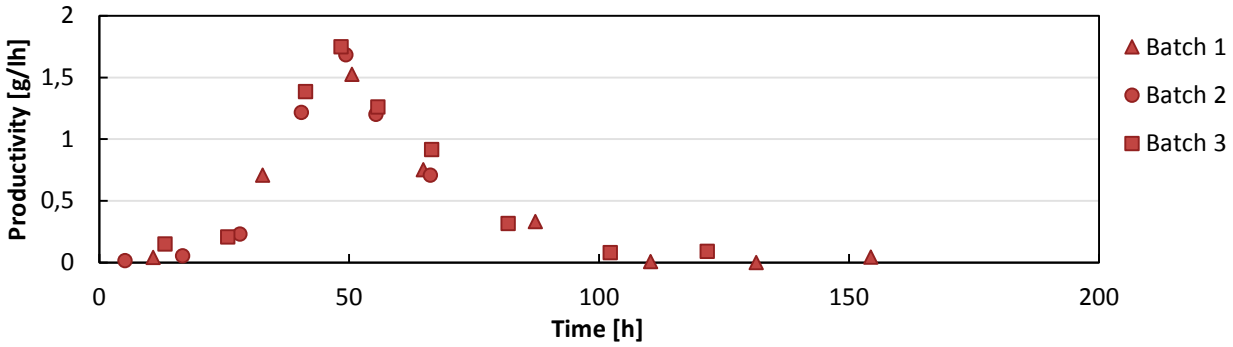

Figure 4-3: SA productivity of the batch fermentations, showing the decrease in productivity as the SA increases

4.2 Continuous fermentation results

Three continuous fermentations were performed during the study, using partial cell recycle. However, the first fermentation showed significant amounts of ethanol, and produced significantly less SA; it could therefore not be used. This was assumed to be either due to an infection or the modified strain reverting back to a more natural strain after several incubation cycles. The subsequent fermentation inoculums were therefore prepared directly from frozen cultures, and ethanol was not detected again.

During the third fermentation the temperature control on the reactor failed, and it had to be operated manually. There were very few samples that could be assumed as steady state. The average mass balance closure of the assumed steady-state samples was, however, very low, at only 84.6%, and the data were therefore assumed to be non-steady state and could not be used.

The second fermentation did, however, succeed in providing multiple steady-state samples at dilution rates of 0.05, 0.10 and 0.15 h^{-1}. The results from the continuous

fermentation with partial cell recycle are given in Figure 4-4 and Figure 4-5, with the steady-state data (as defined in Section 3.6.2) represented as solid markers. The KOH dosing flow rate, which was used to determine whether samples were considered to be at steady state, can be seen in Figure 4-6.

A bleed stream was used to remove a portion of the cells, to prevent dead biomass from accumulating. The flow rate of the bleed stream was set to approximately 11% of the feed stream, with the remainder passing through the hollow fibre filter. The average bleed rate can be seen in Figure 4-4 and Figure 4-5, given in the units of dilution rate (h^{-1}).

In an attempt to increase the cells in the reactor (300 h into the fermentation), the reactor medium was drained through the filter to a volume of about 150 mL, keeping the cells in the reactor. The reactor was then refilled quickly in order to decrease the SA concentration and increase the glucose concentration to allow better cell growth. This had almost no effect on the DCW, although it can be seen in Figure 4-6 as a sudden spike in the KOH dosing.

The DCW was not, however, steady at many points during fermentation at a set dilution rate. This was most obvious in the period following a change in dilution rate. Although the DCW did not reach steady-state conditions, the SA concentration and KOH were steady for long periods, even with significant changes in DCW. The DCW was therefore not used to determine which points could be seen as steady state.

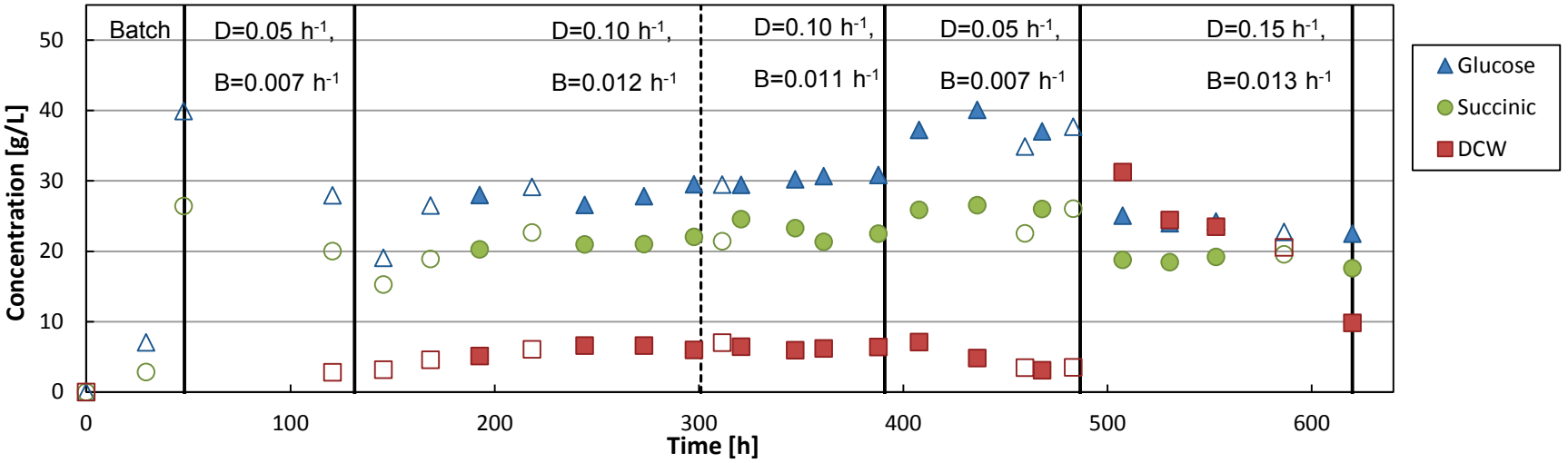

Figure 4-4: Continuous fermentation results, showing the glucose consumed, succinic acid concentration and DCW concentration. Steady-state data are given as solid markers, whereas non-steady-state data are given as markers without a fill

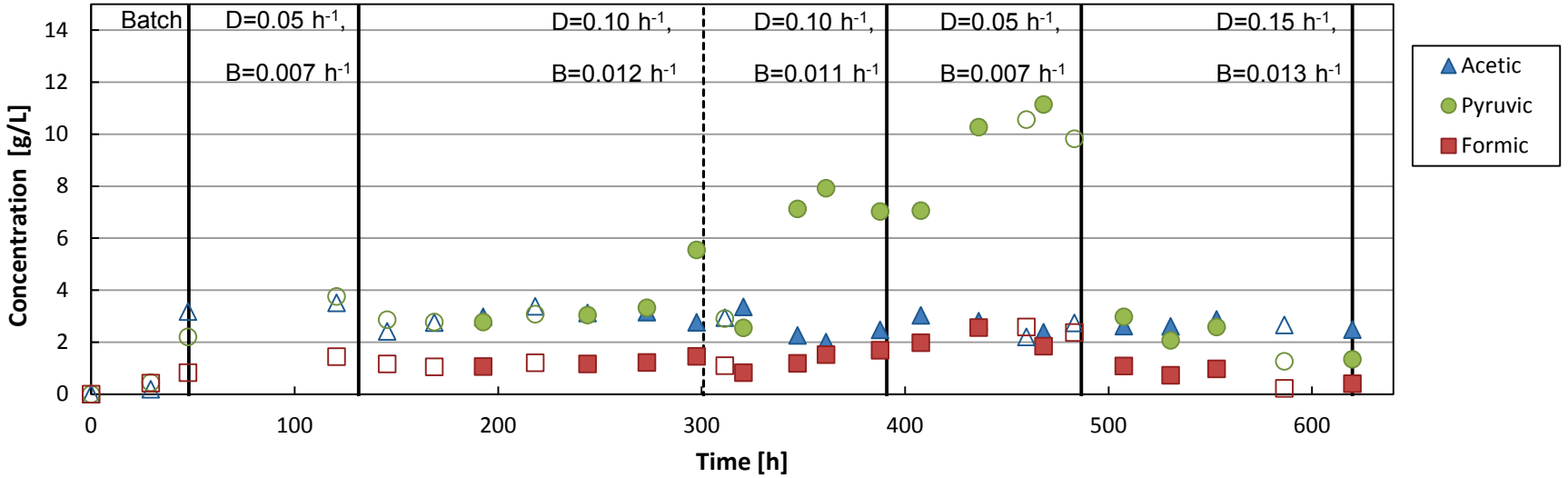

Figure 4-5: Continuous fermentation byproduct results, showing the acetic, pyruvic and formic acid concentrations. Steady-state data are given as solid markers, whereas non-steady-state data are given as markers without a fill

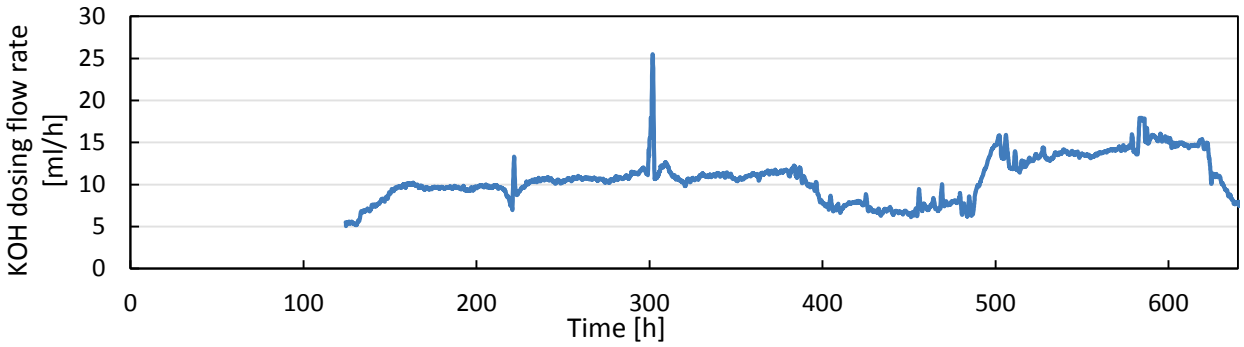

Figure 4-6: KOH dosing rate used in determining whether sample points can be considered as steady state

Since multiple samples were taken at every specific dilution rate, the results are given as an average with a standard deviation in order to better evaluate the differences between dilution rates. The average results of certain metabolites, as well as the average yields and closures, can be seen in Table 4-3. The average SA, FA and PA concentrations are shown in Figure 4-7 in order to illustrate the relative decrease of the metabolites as the dilution rate increased.

Table 4-3: Average continuous fermentation results at different dilution rates, with standard deviation

Dilution rate $[h^{-1}]$	**Closure** [%]	**SA** [g/L]	**AA** [g/L]	**DCW** [g/L]	**Y_{SP}** [g/g]
0.05	94 ± 4	26.2 ± 0.4	2.7 ± 0.30	5.0 ± 1.0	0.69 ± 0.03
0.10	95 ± 4	22.0 ± 1.4	2.8 ± 0.48	6.2 ± 1.0	0.76 ± 0.04
0.15	105 ± 6	18.5 ± 0.7	2.6 ± 0.16	22.3 ± 9.0	0.77 ± 0.02
Average	98 ± 5	22.2 ± 0.8	2.7 ± 0.38	11.2 ± 3.6	0.74 ± 0.03

A mass balance was performed on all the data points, and the average closure of each dilution can be seen in Table 4-3. The closure of the mass balance did increase as the dilution rate increased, with an average closure of 105% at a dilution rate of 0.15 h^{-1}. The closure above 100% suggests that an additional carbon source is present. This might be due to nutrients released from the lysis of biomass caused by the overshoot in cell concentration when switching to a higher dilution rate.

The closure below 100% suggests that more glucose was consumed than needed to account for metabolite and biomass production. Some of the additional glucose consumed might be due to biomass that adhered to the top of the reactor, which was not accounted for in the DCW samples, leading to a DCW value lower than that actually produced. Another reason might be that parts of lysed cells were not detected in the DCW measurement.

Even with the decrease in SA concentration, the SA productivity increases significantly as the dilution rate increases, as seen in Figure 4-8.

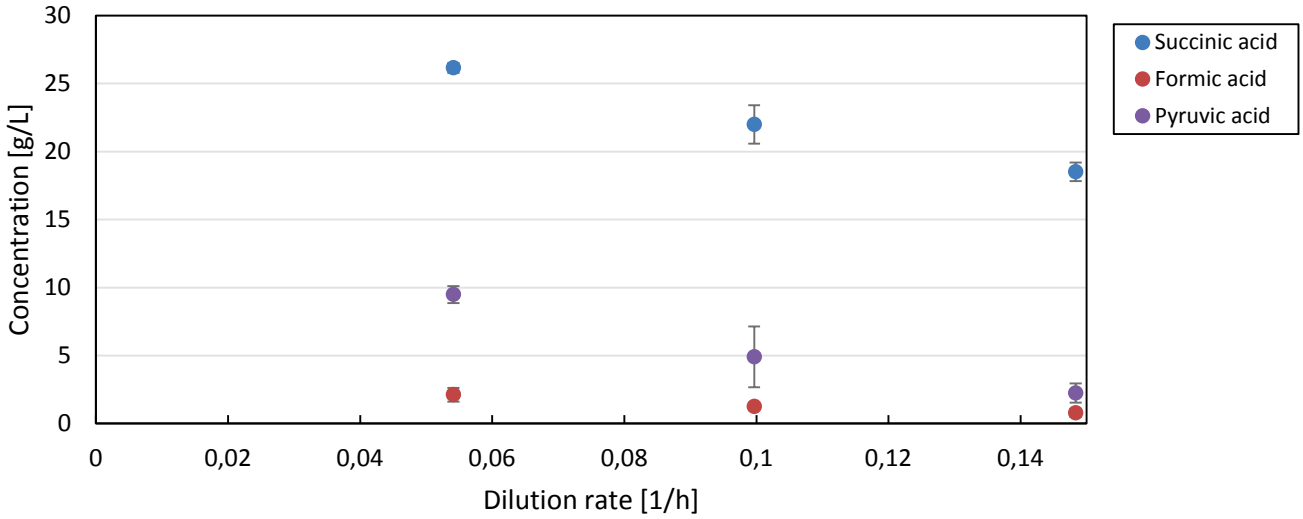

Figure 4-7: Average metabolite concentrations from the continuous cell recycle fermentations, with the error bars representing the standard deviation

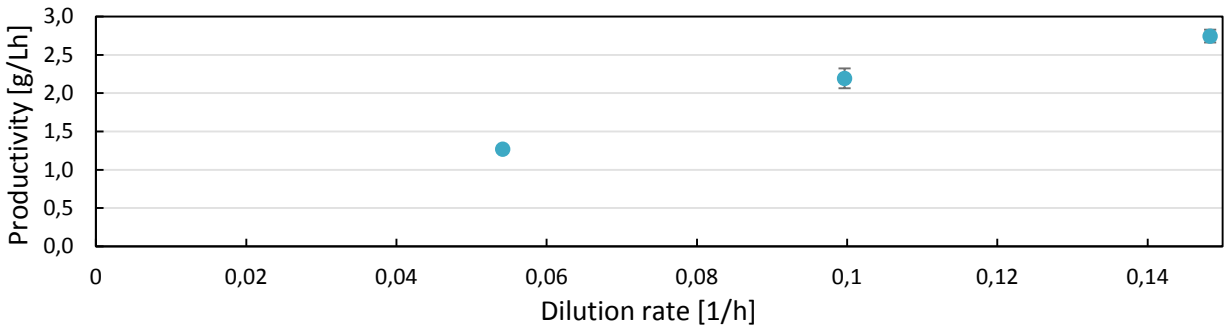

Figure 4-8: SA productivity obtained during the continuous cell recycle fermentation, with the productivity increasing significantly as the dilution rate increases

4.3 Metabolic flux analysis of continuous fermentations

In order to better evaluate the results, a metabolic flux analysis was done on the results of the continuous cell recycle fermentation. The results can be seen in Table 4-4. They are given as the ratio of various fluxes, as explained in Section 3.6.3. The units of all the ratios

are either cmol/cmol or g/g, since these ratios all relate the flux of a molecule to one product divided by the total flux of the same molecule.

To obtain the maximum theoretical yield of 1.12 g/g, all of the pyruvate has to be converted only through pyruvate dehydrogenase, and all the acetyl-CoA needs to be converted to isocitrate instead of acetic acid. From the flux analysis, Table 4-4, it was found that the fraction of pyruvate converted through the pyruvate dehydrogenase complex, rather than pyruvate formate lyase (Pyr_{pdh}, Section 3.6.3), increased significantly as the dilution rate increased, reducing formic acid concentrations. The increased pyruvate dehydrogenase activity also led to an expected drop in the fraction of pyruvate excreted (Pyr_{out}).

Table 4-4: Results from metabolic flux analysis as described in Section 3.6.3

Dilution rate [h^{-1}]	PEP_{pyr} [cmol/cmol]	$ACoA_{cit}$ [cmol/cmol]	Pyr_{pdh} [cmol/cmol]	Pyr_{out} [cmol/cmol]
0.05	0.43 ± 0.004	0.200 ± 0.01	0.19 ± 0.09	0.65 ± 0.04
0.10	0.38 ± 0.035	0.196 ± 0.02	0.50 ± 0.17	0.47 ± 0.15
0.15	0.34 ± 0.021	0.187 ± 0.01	0.68 ± 0.10	0.31 ± 0.07
Average	0.38 ± 0.020	0.19 ± 0.015	0.46 ± 0.12	0.48 ± 0.09

The value of PEP_{pyr} shows the fraction of PEP that enters the start of the oxidative branch of the TCA cycle, whereas $ACoA_{cit}$ shows the fraction of acetyl-CoA that is then finally converted to SA, rather than AA. The values of PEP_{pyr} and $ACoA_{cit}$ therefore show how much and how effectively the oxidative branch of the TCA cycle is used, with regard to SA production.

4.4 Discussion

4.4.1 Cell growth and viability

The decrease in cell growth and the lysis of cells were problematic during fermentations. From Figure 4-1 it can be seen that in batch fermentations the DCW decreases at an SA concentration of around 25 g/L. Since some cell death is usually expected, the DCW value is typically higher than the dry weight of the active cells due to the dead cell mass. The decrease in DCW therefore implies that lysis occurs during the fermentation and that the rate of cell death and lysis exceeds the rate at which cells are produced. From the

significant decrease in DCW, it can be assumed that cell growth is severely inhibited at high SA concentrations.

Relatively high cell densities were obtained during the continuous cell recycle fermentations, seen in Table 4-3, with the maximum DCW (at a dilution rate of 0.15 h^{-1}) reaching 31.3 g/L, 13 times higher than the highest DCW obtained during batch runs. The high DCW obtained was, however, temporary, due to the reduced SA concentration after the dilution rate had been changed from 0.05 to 0.15 h^{-1}. However, the severe inhibition of biomass growth at higher SA concentrations can be seen once again in Figure 4-4 at two points: first, the decrease in biomass after the switch to a lower dilution rate (from 0.10 to 0.05 h^{-1} at t = 390 h) and, secondly, after the DCW overshoot due to the decrease in SA concentration when switching to a higher dilution rate (from 0.05 to 0.15 h^{-1} at t = 470 h). At the point at which the dilution rate was increased from 0.05 to 0.15 h^{-1}, the DCW increased drastically from 3.5 to 31 g/L, but then dropped steadily for more than 100 h. Surprisingly, the SA concentration stayed remarkably constant at an average of 18.5 g/L, even as the DCW dropped to a value of 9.8 g/L in the last sample – less than a third of the initial DCW after the switch to a dilution rate of 0.15 h^{-1}. It is therefore likely that a significant portion of the DCW was due to dead cells trapped in the cell recycle reactor, with the DCW slowly decreasing as the cells lysed or were washed out through the bleed stream.

The DCW can therefore not adequately describe the viable cell concentration because, depending on the time required before the cells lyse, it might include significant dead cell mass. Furthermore, during batch fermentations, Figure 4-1, the SA productivity drops to nearly zero near the end of the fermentation, even though there is still a significant amount of biomass in the reactor. This implies that not only is the cell growth limited by product inhibition, but the SA productivity per DCW is also inhibited. This could imply that the dominant production mode is strongly related to growth.

During continuous fermentations, the inhibition of biomass growth results in biomass dying off until an equilibrium is established between the growth rate, the cells removed through the bleed stream and the death rate with subsequent lysis. This decrease to an equilibrium can be seen most clearly in Figure 4-4, after the switch to a lower dilution rate (from 0.10 to 0.05 h^{-1} at t = 390 h), when the DCW decreases up to a point and then remains relatively constant (at t = 460 h).

The SA titre is therefore limited to concentrations where the net growth rate is equal to the rate at which cells are removed through the bleed stream. Even at full recycle, the SA titre will be limited by the SA concentration where the growth rate is equal to the death rate. From batch runs it is evident that the growth rate decreases significantly above an SA concentration of around 25 g/L.

4.4.2 Comparison with previous studies

While using *E. coli* KJ 122 with the same medium, Jantama *et al*. (2008) reported high SA yields of 0.89 g/g up to 0.96 g/g, and SA titres of up to 82 g/L. The only significant difference in their fermentation methods was the use of K_2CO_3 and bicarbonate to supply CO_2.

The batch fermentations done in this study reached an average maximum SA concentration of 52.2 g/L, which is significantly less than the 82 g/L reported by Jantama *et al*. (2008), using the same strain of *E. coli*. The SA yield, during batch runs, of 0.85 g/g is close to the lowest yield of 0.89 g/g reported by Jantama *et al*. (2008), although this is still significantly lower than the highest yield of 0.96 g/g reported. Due to the relatively large sample sizes, significant amounts of formate and pyruvate were removed during fermentation. This gives one possible explanation for the lower yields, since the formate and pyruvate were not allowed to react further and produce SA.

Van Heerden and Nicol (2013) performed chemostat fermentations using *E. coli* KJ 134, a similar strain of *E. coli* that differs from KJ 122 by only one genetic modification, namely the inactivation of phosphotransacetylase, in order to reduce acetate formation. Although Jantama *et al*. (2008), using *E. coli* KJ 134, reported a 4% higher SA yield, and a 10% lower productivity, the two strains can still reasonably be compared.

During chemostat fermentations, Van Heerden and Nicol (2013) obtained a maximum chemostat productivity of 0.87 g/L/h at a dilution rate of 0.093 h^{-1}, with an SA concentration of 9.3 g/L. A maximum SA concentration of 18 g/L was obtained at a dilution rate of 0.021 h^{-1} with a productivity of 0.38 g/L/h. At a dilution rate of 0.146 h^{-1} the SA concentration obtained was only 5 g/L. From these chemostat results it is obvious that the cell recycle reactor offered a large improvement in maximum titre and productivity, even when taking into account the average results at the different dilution rates, with values of 26.2 g/L and 2.74 g/L/h respectively.

The maximum yield of 0.77 g/g obtained by Van Heerden and Nicol (2013) was exactly the same as the average yield achieved at a dilution rate of 0.15 h^{-1} using a cell recycle reactor.

The cell recycle reactor, using *E. coli* strain KJ 122, achieved relatively high SA yields, even when compared with a strain of *E. coli* (KJ 134) that reportedly achieved higher yields (Jantama *et al*., 2008).

Balzer *et al*. (2013) reported high SA yields of approximately 1.0 g/g using the modified *E. coli* strain SBS550MG-Cms243(pHL413KF1) in an anaerobic fed-batch bioreactor process, with a succinate production rate of 2 g/L/h and an SA titre of around 25 g/L. This yield is significantly higher than that obtained during this study, and the productivity is close to that obtained during cell recycle fermentation at a dilution rate of 0.1 h^{-1} with similar titres. The fermentations by Balzer *et al*. (2013) were, however, done using a complex medium, with high concentrations of tryptone and yeast extract, as well as an initial aerobic fermentation period. It is therefore difficult to compare the results of this study directly with those of Balzer *et al*. (2013).

4.4.3 Metabolic product distribution

Throughout the fermentations pyruvate, formate and acetate formed as byproducts. The accumulation of pyruvate is probably due to a metabolic overflow from glycolysis (Jantama *et al*., 2008). The formate formed is most likely due to some pyruvate formate lyase activity, even though the pyruvate formate lyase was inactivated. A possible explanation for the acetate that forms is that excess acetyl~CoA is converted to acetyl~P which is then converted to acetate by unspecified reactions. These could include the phosphorylation and dephosphorylation of proteins, spontaneous hydrolysis and other reactions (Jantama *et al*., 2008).

In the batch fermentations, the pyruvate and formate concentrations started to decrease significantly at approximately 60 h into the fermentation, as seen in Figure 4-2. This decrease in concentration occurred shortly after the DCW concentration and SA productivity started to decrease (50–55 h into the fermentation).

The decrease in formate is most probably due to the formate being metabolised by formate dehydrogenase, to produce additional NADH. The decrease in pyruvate is most probably due to pyruvate being metabolised to SA and AA, which produces more NADH. This is the most likely reason for the lower final yield observed in Batch 2, Table 4-2, since the pyruvate and formate concentrations were still relatively high.

During continuous fermentations the acetic acid concentration stayed remarkably constant at all dilution rates, at a value of around 2.7 g/L, with a standard deviation of only 0.38 g/L,

as seen in Table 4-3. This suggests a shift in the metabolic pathways used, since the other metabolites did change.

The SA concentration decreases slightly as the dilution rate increases, Figure 4-7, which is expected in continuous fermentation. The average SA yields obtained (Table 4-3) increased as the dilution rate increased (0.77 g/g at D = 0.15 h^{-1} and 0.69 g/g at D = 0.05 h^{-1}). The increase in yield is probably due to the significant decrease in formic and pyruvic acid concentrations, shown in Figure 4-7.

From the metabolic flux analysis (Table 4-4), the value of Pyr_{pdh} increased significantly at higher dilution rates (from 0.19 to 0.68 cmol/cmol). This suggests an increase in pyruvate dehydrogenase activity, increasing the amount of NADH produced in the oxidative branch of the TCA cycle. Due to the additional NADH produced, a higher fraction of the PEP can be converted to SA through the reductive branch of the TCA cycle (seen in the reduction of PEP_{pyr} in Table 4-4), thus increasing the SA yield. The increased *pdh* activity also decreased the fraction of pyruvate that was excreted (Pyr_{out}), instead of being converted to acetyl-CoA, further increasing the yield of SA since less carbon is lost through excreted pyruvate.

Although there is evidence that pyruvate dehydrogenase (*pdh*) can be active under anaerobic conditions, it is primarily active under aerobic conditions (Blankschien, Clomburg & Gonzalez, 2010). No CO_2 is added to the feed medium, and the medium is in contact with air; therefore dissolved oxygen is present in the feed. The CO_2 flow rate is kept constant at all dilution rates, and at higher dilution rates, the oxygen in the feed might not be displaced quickly enough by the CO_2 in the reactor, resulting in microaerobic conditions. This gives a possible explanation for the increased *pdh* activity at higher dilution rates.

Unfortunately, only a small fraction of acetyl-CoA is converted to citrate ($ACoA_{cit}$), (approximately 20% of the total acetyl-CoA formed), resulting in significant amounts of acetate being formed and thus decreasing the overall yield far below the theoretical maximum.

4.4.4 Productivity: Batch fermentation compared with continuous fermentation

The highest instantaneous SA productivity during batch fermentations (a productivity of around 1.7 g/L/h) occurred at an SA concentration of around 22 g/L, slightly before the biomass concentration started decreasing. This is not, however, an accurate representation of the overall productivity of a batch fermentation. The overall productivity and yield of the

batch runs was calculated by setting the end time of the run at the point when the SA reaches 95% of the maximum SA concentration, so as not to include the low productivity at the final SA concentration. Batch 1 and Batch 3 were used since Batch 2 did not reach the maximum SA concentration, with the average overall productivity then calculated as 0.59 g/L/h. Using the same point, an average yield of 0.83 g_{SA}/g_{gluc} was calculated.

During continuous fermentation, even with the decrease in SA concentration, the SA productivity increases significantly as the dilution rate increases, as seen in Figure 4-8. The slope does, however, decrease slightly from the dilution rate of 0.1 to 0.15 h^{-1}. The maximum productivity obtained was 3 g/L/h, at a dilution rate of 0.15 h^{-1}, with the average being slightly lower. This suggests that higher productivities (than the 2.8 g/L/h obtained at a dilution rate of 0.15 h^{-1}) are possible at higher dilution rates.

Even with the significant limitation on continuous operation caused by the SA inhibition, the continuous cell recycle fermentations had production rates significantly higher than the batch fermentations. Even at a dilution rate of only 0.05 h^{-1}, the average productivity of 1.27 g/L/h is close to the maximum productivity during batch runs, namely 1.7 g/L/h. When the overall production rate of the batch runs is considered, this difference is even more significant. The average overall productivity during batch runs, at a value of 0.59 g/L/h, is significantly lower than the productivity during continuous cell recycle fermentation, even at low dilution rates. The average productivity at a dilution rate of 0.15 h^{-1} is 4.6 times higher than the overall productivity of the batch fermentations, and almost twice the maximum instantaneous productivity of the batch fermentations.

A major concern with continuous production is the low titre obtained since this will lead to significantly higher downstream processing costs. A further disadvantage is that the yields obtained during continuous cell recycle fermentation (0.69 to 0.77 g/g) are significantly lower than that of batch runs (0.85 g/g).

5 Conclusions

In this study the succinic acid (SA) productivity, yield and titre of *Eschericia coli* KJ 122 were evaluated under high cell density fermentation (HCDF) conditions. The HCDF data were analysed using metabolic flux analysis in order to obtain a better understanding of the metabolic pathways that are active during continuous fermentation. Batch fermentations were performed for the purposes of comparison and to investigate the productivity, yield and titre that could be obtained.

The highest continuous volumetric productivity of 3 g/L/h was achieved at the highest dilution rate (0.15 h^{-1}) at an SA titre of 19 g/L, and was five times higher than the overall batch productivity where a final titre of 56 g/L was measured. This shows that continuous cell recycle fermentation could significantly increase the volumetric productivity, although at the cost of a lower titre. Unfortunately, severe product inhibition, at SA concentrations above 25 g/L, makes continuous high titre production unfeasible and limits the cellular concentration in the fermenter due to cell death and subsequent cell lysis. Therefore, although temporary high dry cell weight was achieved, the biomass died off until an equilibrium was established between the cell growth, cell death and cells removed through the bleed stream.

The SA yields obtained during batch fermentation were, however, superior to all the SA yields obtained during continuous cell recycle fermentations. This was due mainly to the utilisation of pyruvate and formate at high SA titres, during late stages of the batch fermentations.

Higher continuous yields were, however, obtained at higher dilution rates. The metabolic flux analysis indicated an increase in pyruvate dehydrogenase activity at higher dilution rates, increasing the SA yields. This led to a decrease in pyruvate excretion, a reduction in the amount of formate formed and an increase in the reductive phosphoenolpyruvate flux towards SA. The maximum average yield obtained during continuous cell recycle fermentation (0.77 g/g) is, nevertheless, significantly lower than that obtained by Jantama *et al*. (2008), which was 0.89 to 0.96 g/g, and far lower than the theoretical yield of 1.12 g/g.

The relatively low titres of the continuous fermentation would increase the downstream processing requirements. Therefore, the low titres and high productivities of continuous cell recycle fermentation would have to be evaluated against the lower productivities and higher

titres achieved in a batch fermentation to determine whether continuous cell recycle fermentation would be economically feasible.

6 References

Balzer, GJ, Thakker, C, Bennett, GN & San, K-Y (2013) "Metabolic engineering of *Escherichia coli* to minimize byproduct formate and improving succinate productivity through increasing NADH availability by heterologous expression of NAD(+)-dependent formate dehydrogenase.," *Metabolic Engineering*, 20, 1–8.

Beauprez, JJ, De Mey, M & Soetaert, WK (2010) "Microbial succinic acid production: Natural versus metabolic engineered producers," *Process Biochemistry*, 45(7), 1103–1114.

Blankschien, MD, Clomburg, JM & Gonzalez, R (2010) "Metabolic engineering of *Escherichia coli* for the production of succinate from glycerol.," *Metabolic Engineering*, 12(5), 409–19.

Borch, E, Berg, H & Holst, O (1991) "Heterolactic fermentation by a homofermentative Lactobacillus sp. during glucose limitation in anaerobic continuous culture with complete cell recycle," *Journal of Applied Microbiology*, 71(1), 265–269.

Chang, H, Yoo, I & Kim, B (1994) "High density cell culture by membrane-based cell recycle," *Biotechnology Advances*, 12, 467–487.

Cheryan, M & Mehaia, M (1983) "A high-performance membrane bioreactor for continuous fermentation of lactose to ethanol," *Biotechnology Letters*, 5(8), 519–524.

Cheryan, M (1998) *Ultrafiltration and Microfiltration Handbook*, 1st ed. Technomic Publishing, Illinois.

Jang, Y-S, Malaviya, A & Lee, SY (2013) "Acetone-butanol-ethanol production with high productivity using Clostridium acetobutylicum BKM19.," *Biotechnology and Bioengineering*, 110(6), 1646–53.

Jansen, M LA & Van Gulik, WM (2014) "Towards large scale fermentative production of succinic acid.," *Current Opinion in Biotechnology*, 30C, 190–197.

Jantama, K, Zhang, X, Moore, JC, Shanmugam, KT, Svoronos, SA & Ingram, LO (2008) "Eliminating side products and increasing succinate yields in engineered strains of *Escherichia coli* C.," *Biotechnology and bioengineering*, 101(5), 881–93.

Kim, M Il (2009) "Continuous production of succinic acid using an external membrane cell recycle system," *Journal of Microbiology and Biotechnology*, 19(11), 1369–1373.

Lee, S, Chang, H, Um, Y & Hong, S (1998) “Bacteriorhodopsin production by cell recycle culture of *Halobacterium halobium*,” *Biotechnology Letters*, 20(8), 763–765.

Lee, C, Gu, M & Chang, H (1989) “High-density culture of *Escherichia coli* carrying recombinant plasmid in a membrane cell recycle fermenter,” *Enzyme and Microbial Technology*, 11(1), 49–54.

Lin, H, Bennett, GN & San, K-Y (2005) “Metabolic engineering of aerobic succinate production systems in *Escherichia coli* to improve process productivity and achieve the maximum theoretical succinate yield.,” *Metabolic Engineering*, 7(2), 116–27.

Martinez, A, Grabar, TB, Shanmugam, KT, Yomano, LP, York, SW & Ingram, LO (2007) “Low salt medium for lactate and ethanol production by recombinant *Escherichia coli* B.,” *Biotechnology Letters*, 29(3), 397–404.

Meynial-Salles, I, Dorotyn, S & Soucaille, P (2008) “A new process for the continuous production of succinic acid from glucose at high yield, titer, and productivity.,” *Biotechnology and Bioengineering*, 99(1), 129–35.

Muffler, K & Ulber, R (2008) “Use of Renewable Raw Materials in the Chemical Industry – Beyond Sugar and Starch,” *Chemical Engineering & Technology*, 31(5), 638–646.

Nielsen, JJJH, Villadsen, J & Lidén, G (2011) *Bioreaction Engineering Principles*, 3rd ed, Springer, New York, 0–8.

Nolasco-hipolito, C, Matsunaka, T, Kobayashi, G, Sonomoto, K & Ishizaki, A (2002) “Synchronized fresh cell bioreactor system for continuous L-(+)-lactic acid production using *Lactococcus lactis* IO-1 in hydrolysed sago starch,” *Journal of Bioscience and Bioengineering*, 93(3), 281–287.

Park, Y, Ohtake, H & Toda, K (1989) “Acetic acid production using a fermentor equipped with a hollow fiber filter module,” *Biotechnology and Bioengineering*, 33(1), 918–923.

Pierrot, P, Fick, M & Engasser, J (1986) “Continuous acetone-butanol fermentation with high productivity by cell ultrafiltration and recycling,” *Biotechnology Letters*, 8(4), 253–256.

Schügerl, K & Zeng, A-P (Eds.) (2007) *Tools and Applications of Biochemical Engineering Science*, Vol. 74, in: *Series: Advances in Biochemical Engineering/Biotechnology*, Springer, Berlin.

Sheldon, RA. (2011) “Utilisation of biomass for sustainable fuels and chemicals: Molecules, methods and metrics,” *Catalysis Today*, 167(1), 3–13.

Song, H & Lee, SY (2006) “Production of succinic acid by bacterial fermentation,” *Enzyme and Microbial Technology*, 39(3), 352–361.

Tashiro, Y, Takeda, K, Kobayashi, G & Sonomoto, K (2005) “High production of acetone-butanol-ethanol with high cell density culture by cell-recycling and bleeding.,” *Journal of Biotechnology*, 120(2), 197–206.

Toda, K (2003) “Theoretical and methodological studies of continuous microbial bioreactors.,” *Journal of General and Applied Microbiology*, 49(4), 219–33.

Van Heerden, CD & Nicol, W (2013) “Continuous and batch cultures of *Escherichia coli* KJ134 for succinic acid fermentation: Metabolic flux distributions and production characteristics.,” *Microbial Cell Factories*, 12(1), 80.

Van Reis, R & Zydney, A (2007) “Bioprocess membrane technology,” *Journal of Membrane Science*, 297(1-2), 16–50.

Vemuri, GN, Eiteman, MA & Altman, E (2002a) “Effects of growth mode and pyruvate carboxylase on succinic acid production by metabolically engineered strains of *Escherichia coli*,” *Applied and Environmental Microbiology*, 68(4), 1715–1727.

Vemuri, GN, Eiteman, MA & Altman, E (2002b) “Succinate production in dual-phase *Escherichia coli* fermentations depends on the time of transition from aerobic to anaerobic conditions.,” *Journal of industrial microbiology & biotechnology*, 28 (6), 325–32.

Werpy, T & Petersen, G (2004) *Top value added chemicals from biomass volume I — Results of screening for potential candidates from sugars and synthesis gas*. Program 76. Washington DC, U.S. Department of Energy Energy Efficiency and Renewable Energy. Available at: http://oai.dtic.mil/oai/oai?verb=getrecord&metadataprefix=html&identifier=ada436528

Yoo, I, Chang, H, Lee, E, Chang, Y & Moon, S (1997) “By-product formation in cell-recycled continuous culture of *Lactobacillus casei*,” *Biotechnology Letters*, 19(3), 237–240.

Zeng, A, Biebl, H & Deckwer, W (1991) “Production of 2, 3-butanediol in a membrane bioreactor with cell recycle,” *Applied Microbiology and Biotechnology*, 34(1), 463–468.

Zhang, X, Jantama, K, Shanmugam, KT & Ingram, LO (2009) “Reengineering *Escherichia coli* for succinate production in mineral salts medium.,” *Applied and Environmental Microbiology*, 75(24), 7807–13.